SECRET
SECURITY INFORMATION

CENTRAL RESEARCH LIBRARY
DOCUMENT COLLECTION

OAK RIDGE NATIONAL LABORATORY LIBRARY
3 4456 0023193 3

ORNL-1359
Progress
5a

DECLASSIFIED
CLASSIFICATION CHANGED TO:
BY AUTHORITY OF: TID-1234
BY: E. Shaw 1/14/61

AEC RESEARCH AND DEVELOPMENT REPORT

SOLID STATE DIVISION

QUARTERLY PROGRESS REPORT

FOR PERIOD ENDING AUGUST 10, 1952

CENTRAL RESEARCH LIBRARY
DOCUMENT COLLECTION
LIBRARY LOAN COPY
DO NOT TRANSFER TO ANOTHER PERSON
If you wish someone else to see this document, send in name with document and the library will arrange a loan.

OAK RIDGE NATIONAL LABORATORY
OPERATED BY
CARBIDE AND CARBON CHEMICALS COMPANY
A DIVISION OF UNION CARBIDE AND CARBON CORPORATION
UCC
POST OFFICE BOX P
OAK RIDGE, TENNESSEE

RESTRICTED DATA
This document contains Restricted Data as defined in the Atomic Energy Act of 1946. Its transmittal or the disclosure of its contents in any manner to an unauthorized person is prohibited.

SECRET
SECURITY INFORMATION

5- Central Res. Lib

ERRATA SHEET

SOLID STATE DIVISION QUARTERLY PROGRESS REPORT FOR PERIOD ENDING AUGUST 10, 1952 ORNL-1359

PAGE NO.	COLUMN NO.	LINE NO.	ERRATA
26	1	11 and 12	*for* 10 ev *read* 10 kev
28	2	16	*for* Dekye-Scherus *read* Debye-Scherrer
37	1	9 through 13	*should read* traps (one shallow electron trap near the bottom of the conduction band, estimated to be approximately 0.05 ev deep, and one deep electron trap below the middle of the forbidden band) and one rather shallow trap (if a second trap
47	2	19	*for* constant *read* constantan
48	1	17	*should read* samples 17A, 19A, 14B, 16A, and 21A were made with
		36	*for* 3A *read* 3B
		45	*should read* The bombardment of samples 17A, 19A, 14B, and 16A was
		48	*for* water-cooled *read* air-cooled
	2	10	*for* 19B *read* 19A, 14B, 16A, and 21A
49	Table 9	21	*for* 2×10^{18} *read* 1×10^{18}
50	Table 10		eleventh number in column ρ_T, *should read* 0.20118 first number column $\rho_{-196.0}$ *should read* 0.19712

[redacted]

ORNL-1359

This document consists of 59 pages.
Copy 5 of 143 copies. Series A.

Contract No. W-7405-eng-26

DECLASSIFIED
CLASSIFICATION CHANGED TO:
BY AUTHORITY OF: TID-1236
BY: 11/14/64

SOLID STATE DIVISION

QUARTERLY PROGRESS REPORT

for Period Ending August 10, 1952

D. S. Billington, Director

Edited by

J. T. Howe

DATE ISSUED

JAN 15 1953

OAK RIDGE NATIONAL LABORATORY
Operated by
CARBIDE AND CARBON CHEMICALS COMPANY
A Division of Union Carbide and Carbon Corporation
Post Office Box P
Oak Ridge, Tennessee

OAK RIDGE NATIONAL LABORATORY LIBRARY
3 4456 0023193 3

[redacted]
CENTRAL RESEARCH LIBRARY
DOCUMENT COLLECTION
LIBRARY LOAN COPY
DO NOT TRANSFER TO ANOTHER PERSON
If you wish someone else to see this document, send in name with document and the library will arrange a loan.

[redacted]

ORNL-1359
Progress

INTERNAL DISTRIBUTION

1. G. T. Felbeck (C&CCC)
2. Biology Library
3. Health Physics Library
4. Metallurgy Library
5-6. Central Research Library
7. Reactor Experimental Engineering Library
8-13. Central Files
14. C. E. Center
15. C. E. Larson
16. W. B. Humes (K-25)
17. L. B. Emlet (Y-12)
18. A. M. Weinberg
19. E. H. Taylor
20. E. J. Murphy
21. E. D. Shipley
22. D. S. Billington
23. F. C. VonderLage
24. R. C. Briant
25. J. A. Swartout
26. S. C. Lind
27. F. L. Steahly
28. A. H. Snell
29. A. Hollaender
30. M. T. Kelley
31. G. H. Clewett
32. K. Z. Morgan
33. J. S. Felton
34. A. S. Householder
35. C. S. Harrill
36. C. E. Winters
37. D. W. Cardwell
38. E. M. King
39. C. P. Keim
40. L. K. Jetter
41. E. J. Boyle
42. W. D. Manly
43. C. D. Susano
44. B. S. Borie
45. R. J. Gray
46. E. E. Stansbury
47. G. P. Smith
48. J. E. Cunningham
49. E. C. Miller
50. W. J. Fretague
51. J. O. Betterton, Jr.
52. R. B. Oliver
53. T. H. Blewitt
54. J. H. Crawford, Jr.
55. W. E. Brundage
56. O. Sisman
57. G. W. Keilholtz
58. J. T. Howe
59. R. H. Kernohan
60. S. E. Dismuke
61. J. C. Wilson
62. W. J. Sturm
63. M. T. Robinson
64. J. W. Cleland
65. K. Lark-Horovitz (consultant)
66. M. C. Wittels
67. R. A. Weeks
68. W. W. Parkinson
69. C. D. Bopp
70. C. D. Baumann
71. J. B. Trice
72. J. G. Morgan
73. G. E. Klein
74. R. G. Berggren
75. D. K. Holmes
76. D. K. Stevens
77. A. J. Miller (Y-12)
78. R. S. Livingston (Y-12)
79. R. J. Jones (Y-12)
80. D. D. Cowen
81. P. M. Reyling

RESTRICTED DATA

This document contains Restricted Data as defined in the Atomic Energy Act of 1946. Its transmittal or the disclosure of its contents in any manner to an unauthorized person is prohibited.

[redacted]

EXTERNAL DISTRIBUTION

82-89. Argonne National Laboratory
90-92. Atomic Energy Commission, Washington
93-96. Brookhaven National Laboratory
97-100. Carbide and Carbon Chemicals Company (Y-12 Area)
101-103. Knolls Atomic Power Laboratory
104-105. General Electric Company, Richland
106. Hanford Operations Office
107-110. Los Alamos
111-112. New York Operations Office
113. Patent Branch, Washington
114-128. Technical Information Service, Oak Ridge
129-132. University of California Radiation Laboratory
133. Massachusetts Institute of Technology (Kaufmann)
134. Battelle Memorial Institute
135-137. North American Aviation, Inc.
138. Westinghouse Electric Corporation
139. Savannah River Operations Office, Wilmington
140-143. Idaho Operations Office (1 copy to Phillips Petroleum)

[redacted]
This docum[redacted] contains Restricted Data as [redacted] Energy Act of 1946. Its transmittal or the disclosure of its contents [redacted] in any manner to an unauthorized person is prohibited.

Reports previously issued in this series are as follows:

ORNL-1025	Period Ending January 31, 1951
ORNL-1095	Period Ending April 30, 1951
ORNL-1128	Period Ending July 31, 1951
ORNL-1214	Period Ending October 31, 1951
ORNL-1261	Period Ending January 31, 1952
ORNL-1301	Period Ending May 10, 1952

[redacted]

This [redacted] contains Restricted [redacted] Ene[redacted] its transmittal or the disclosure of its contents in any manner to an unauthorized person is prohibited.

[redacted]

CONTENTS

	Page
PART I. SECRET PROJECTS	1
SUMMARY	3
RADIATION METALLURGY	5
Creep Under Irradiation	5
Effect of Radiation on Thermocouples	7
MTR Creep Experiments	9
Radiation Effect on Electronic Equipment	9
Impact Tests on Irradiated Metals	9
ENGINEERING PROPERTIES	10
Neutron Measurements	10
Nuclear-Reaction Studies	14
ORNL Graphite Reactor Liquid-Metals Loop	14
Standardization of Liquid-Metal Flowmeters	15
MTR Fluoride-Fuel Loop	18
LITR Sodium Stress-Corrosion Loop	18
FUSED SALTS	19
Zirconium-Base Eutectic Salts	19
Liquid-Fuels Irradiation in the MTR	19
Xenon-135 in Fluoride Fuels	19
Radiation Stability of Copper Phthalocyanine	20
Irradiation Facility in Hole HB-6 of the LITR	21
Dynamic Radiation-Damage Studies	21
CRYSTAL PHYSICS	24
ANP Reactor Fuel-Element Corrosion Under Proton Irradiation	24
Effects of Thermal Gradient Across Bombarded Fuel Elements	24
Investigation of the Causes of Radiation Corrosion	25
Hardening and Embrittlement of Metals	26
Metallographic Equipment	26
Thermal Conductivity of Structural Materials	27
Cryostat for Low-Temperature Studies	27
SPECIAL PROJECTS	28
Materials Irradiation	28
Effect of Neutron Irradiation on Miscellaneous Materials	28
PART II. UNCLASSIFIED PROJECTS	31
SUMMARY	35

RESTRICTED DATA

This [redacted] Restricted Data as defined in the Atomic Energy Act of 1946. Its transmittal or the [redacted] ts in [redacted] manner to an unauthorized person is prohibited.

SOLID STATE REACTIONS 36
Low-Temperature Bombardment of Germanium 36
Magnetic Susceptibility of Germanium Semiconductors 39
Hall and Magnetoresistance Effects in Metals 39
Radiation Effects in Ionic Crystals 40

ENGINEERING PROPERTIES 41
Physical Properties of Irradiated Plastics and Elastomers 41
X-ray Studies of Plastics and Elastomers 41

CRYSTAL PHYSICS 46
Effects of Reactor Irradiation on the Properties of Copper Single Crystals 46
X-ray Work 51

[redacted]
This document [redacted] Data as defined in the [redacted] Energy Act of 1946. [redacted] in any [redacted] person is prohibited.

Part I

[redacted] PROJECTS

SOLID STATE DIVISION QUARTERLY PROGRESS REPORT

SUMMARY

RADIATION METALLURGY

Creep Under Irradiation. Increasing the pre-irradiation anneal temperature from 1650 to 1700°F appears to reduce the adverse effect of neutron bombardment on the creep rate of Inconel at 1500°F and 1500 psi. Up to at least 50 hr, the amount of creep experienced in bench tests and in-pile tests is of the same magnitude.

Effects of Radiation on Thermocouples. The leakage resistance of glass-insulated duplex chromel-alumel thermocouple wires has been found to decrease with irradiation when used in a stagnant helium atmosphere. After 40 hr in the LITR and at a control temperature of 1500°F, these thermocouples indicated a temperature 100°F below that of a platinum resistance thermometer that was wound on alumina spacers. The leakage resistance between the chromel and alumel wires dropped continuously from 11 megohms to 0.7 megohm in 145 hours.

The stagnant helium was replaced by moving air and an intercalibration of chromel-alumel and platinum-rodium thermocouples was made. After a week at 1500°F, the difference in reading between these couples was only 5°F. A resistance thermometer made of platinum wire wound in a quartz sleeving indicated about 30°F decrease in temperature; the wire may have been contaminated by silicon in this case.

The decreases observed in the leakage resistance of duplex thermocouple wire is thought to be caused by carbonization in an inert atmosphere of the organic binder used in the glass insulation. The products appear to be carried off as gases by the air.

MTR Creep Experiment. Three bellows-loaded creep rigs and a device for calibrating the bellows are being built. An alternate dead-weight-loaded apparatus is also being designed.

Radiation Effects in Electronic Equipment. No change has been observed in the four units of electronic equipment that were irradiated for over 100 hr in the bulk shielding facility. An interim report is being prepared at Wright Field.

Impact Tests on Irradiated Metals. The remotely controlled impact tester has been modified to obtain faster operation and better positioning of subsize Izod test specimens. Cooling facilities have also been added to permit impact tests of specimens at −190 to +80°C. Impact tests have been made on unirradiated titanium at temperatures of 30 to −170°C. Specimens of normalized SAE 1040 steel and type 304 ELC stainless steel are being irradiated in the ORNL graphite reactor and the LITR.

ENGINEERING PROPERTIES

Neutron Measurements. Neutron measurements were completed in the LITR, hole HB-2. Curves of thermal-flux traverses, neutron energy spectra, and integrated fluxes above threshold energies are given. Similar neutron spectral measurements are given for the ORNL graphite reactor, hole 1867.

Nuclear Reaction Studies. A study has been made of the reactions $Cl^{35}(n,\alpha)P^{32}$ and $N^{14}(n,p)C^{14}$. The cadmium ratio for the $Cl^{35}(n,\alpha)P^{32}$ reaction was determined to be unity as a result of measurements made in hole 1867 of the graphite reactor. This indicates that the reaction is endoergic. The effective threshold reaction was calculated to occur at approximately 0.6 Mev for reactor-type neutron spectra. This data agrees with that given by the *Handbook of Chemistry and Physics* and is contrary to that reported by Josef Mattauch.

The $N^{14}(n,p)C^{14}$ reaction was used to check the neutron spectrum in the LITR, hole HR-1. From the spectral function obtained, together with the cross section as a function of energy, the quantity of C^{14} produced for a given exposure of Be_3N_2 wrapped in cadmium was estimated. The experimental results were in excellent agreement with the predicted production, especially since the principal activation of the reaction occurs in the spectral region of most uncertainty.

ORNL Graphite Reactor Liquid-Metals Loop. Investigation was made as to the cause of plugging in the liquid-sodium loop. A fine, powdery material was found to be blocking the tube in the cool zone. This material contained less chromium and less iron but more nickel than normal for Inconel. The plugging may have been caused by mass transfer from the hot to the cold zone or it may be attributed

to an insoluble metallic residue from the sodium reaction with the metal oxides on the tubing surface. Metallurgical comparison of unirradiated tubing with sections taken from the loop shows that there is little effect caused by flowing sodium and no appreciable change in the wall thickness of the loop tubing.

Two new loop assemblies have been built and tested. Both failed at the overlap of the weld joining the tube to the end block. To eliminate the possibility that surface oxides at the start of the weld may be covered by the overlap at the end of the weld, the next welds will be backed with a nickel-palladium braze.

An ionization chamber is being calibrated for use in measuring the activity of the circulating sodium for comparison with the activity previously measured for the circulating lithium.

Standardization of Liquid-Metal Flowmeters. A standard type of flowmeter has been designed and tested. Duplicate cells of the same size and material differed by not more than 1% in calibration. Cells made of Inconel or stainless steel also showed little difference in calibration.

MTR Fluoride-Fuel Loop. Design is nearing completion on the components of a fluoride-fuel loop to be operated in the MTR. A description of the apparatus will be presented in detail in the next quarterly report.

LITR Sodium Stress-Corrosion Loop. Trouble was experienced in inserting the stress-corrosion loop apparatus in the LITR, hole HB-2. A wooden dummy plug was fitted to the hole and a new plug made to the same dimensions. In addition to the plug trouble, a rod mounted within the stress-corrosion specimen to reduce the flow area was found to have sagged so that it touched the wall of the specimen. This rod was replaced with a tube made in the form of a uranium-stainless steel sandwich, plugged at both ends, and supported by a spider. The Metallurgy Division expects to obtain information from this tube that will relate to the behavior of fuel-bearing assemblies.

FUSED SALTS

Zirconium-Base Salts. No pressure build-up or serious radiation damage effects have been noted in the studies of zirconium-base salts.

Liquid-Fuels Irradiation in the MTR. The apparatus for the irradiation of liquid fuels in an MTR beryllium A piece has been shipped. Installation is in process at the site.

Xenon-135 in Fluoride Fuels. Two irradiations in the ORNL graphite reactor, hole 12, were made of No. 2 fluoride fuel in order to collect the Xe^{135} produced in the fuel. In one run the helium carrier gas was bubbled through the fuel and in the other helium merely passed over the surface. The xenon was collected in a charcoal trap cooled by dry ice-acetone. The amount of Xe^{135} collected was determined by counting in a 4π-geometry high-pressure chamber.

Conclusions made on the basis of data obtained are: (1) Fission-produced iodine does not appear in the fluoride salt in a volatile form such as I_2 or IF_5. Iodine probably occurs as the simple iodide ion, I^-. (2) Xe^{135} probably diffuses very slowly in the fluoride melt. Computations will be made to provide a check on the experimental results.

Radiation Stability of Copper Phthalocyanine. Organic compounds are usually considered to be too unstable for reactor applications. Copper phthalocyanine ($C_{32}H_{16}N_8Cu$) seems to be among the most stable organic substances at elevated temperatures. A batch of this compound was obtained, but x-ray diffraction studies indicated that it was the unstable alpha modification. A small quantity of the stable beta modification was prepared by mulling the alpha form in cyclohexanol.

Irradiation Facility Hole HB-6 of the LITR. A facility has been installed in the LITR, hole HB-6, to permit exposure of small samples. It is necessary to remove only a small portion of the plug when changing samples.

Dynamic Radiation-Damage Studies. A rocking fuel-irradiation capsule has been designed in such a way that the fuel can be alternately heated in the presence of irradiation and cooled in a non-irradiated portion; this will simulate the actual conditions expected in the ARE. The experiment will be run in the LITR, hole HB-2. Methods of calculating the flux pattern within the capsule have been worked out and numerical values will be obtained as soon as the geometrical details have been decided.

CRYSTAL PHYSICS

ANP Reactor Fuel-Element Corrosion Under Proton Bombardment. The proton beam of the Y-12 86-in. cyclotron has been increased from 20 to 22.5 Mev. Three 8-hr bombardments have been

made of Inconel capsules containing fuel eutectic No. 21 at 815°C. Analysis and inspection has been completed on only one of the specimens, but it appears that the increase in proton energy has increased the depth of corrosion by 0.0015 inch. Although the evidence indicates that corrosion is enhanced by proton bombardment, the rate in the materials under study does not seem sufficient to prevent their use in a reactor.

Thermal Gradient Across Bombarded Fuel Elements. All fuel elements bombarded in the Y-12 cyclotron have been subjected to large temperature gradients between the bombarded areas and the heat-removal areas whereas all control specimens have been subjected to uniform heating in a furnace. To make certain that this difference in conditions was not responsible for the increased corrosion observed in the irradiated specimens, a control sample was made up in which the front face was heated to 815°C, but the rear face of the specimen was maintained at 40°C. No mass transfer type of corrosion caused solely by thermal gradient was found.

Investigation of the Causes of Radiation Corrosion. It is desirable to determine whether radiation corrosion is caused by the ionization or by the knock-on process. An absorbing wedge inserted in the proton path ahead of the target should produce bombarding protons of all energies from 22.5 Mev to zero. An examination of the specimen should then reveal which type of bombardment increases the corrosion rate the most. Another method would be to mount a rotating graphite disk of continuously varying thickness in the proton beam, but difficulty is expected in activating an electric motor in the 9000-gauss magnetic field of the cyclotron for this method.

Hardening and Embrittlement of Metals. Increases of 20 Tukon numbers have been noted in polycrystalline copper specimens as a result of 22.5-Mev proton bombardment. Bombardment of aluminum for 100 μamp-hr has not been sufficient to produce more than barely detectable hardening.

Metallographic Equipment. A Vickers projection metallograph equipped with a carbon arc and point tungsten lamp as alternate light sources, and polarizer and analyzer filters has been temporarily set up in Building 3025. Instrumentation for remotely controlled equipment for preparing and photographing radioactive specimens is nearing completion.

Thermal Conductivity of Structural Materials. Absolute thermal-conductivity measurements have been made as a function of temperature on an ARE heat-treated specimen. These measurements were made before irradiation, during irradiation in hole HB-3 of the LITR, and after irradiation. Measurements were taken over a period of two weeks at temperatures from 130 to 825°C. Before- and after-irradiation conductivity was the same within the accuracy of the measurements, and there was no change in conductivity noted as a function of irradiation.

Cryostat for Low-Temperature Studies. A cryostat has been designed for use between temperatures of 2 and 90°K to investigate the effect of neutron irradiation on the crystal lattices of dielectrics, semiconductors, and metals. Measurements of thermal and electrical conductivity will be made before and after irradiation.

RADIATION METALLURGY

CREEP UNDER IRRADIATION

W. W. Davis J. C. Wilson
J. C. Zukas

Increasing the annealing temperature of Inconel from 1650 to 1700°F appears to reduce the adverse effect of neutron bombardment on the creep at 1500°F and 1500 psi that was reported earlier.[1] The bench and in-pile results after annealing at 1700°F are depicted by the two lower curves in Fig. 1; the other four curves, reported last quarter,[1] are shown for comparison. Although the difference in behavior is attributed to the heat treatment, there was a difference in the manner of annealing that could have been partly responsible. The 1650°F anneals were carried out *in situ* and only the gage length was exposed to the desired temperature, so that some long-time metallurgical changes in and beyond the fillets could have occurred. During the 1700°F anneals, the full length of the specimen was heated in a large furnace.

The possibility that some metallurgical change, such as grain growth, caused the increased creep after the 1650°F anneal is not unlikely in Inconel.

[1] *Solid State Quar. Prog. Rep. May 10, 1952*, ORNL-1301 (in press).

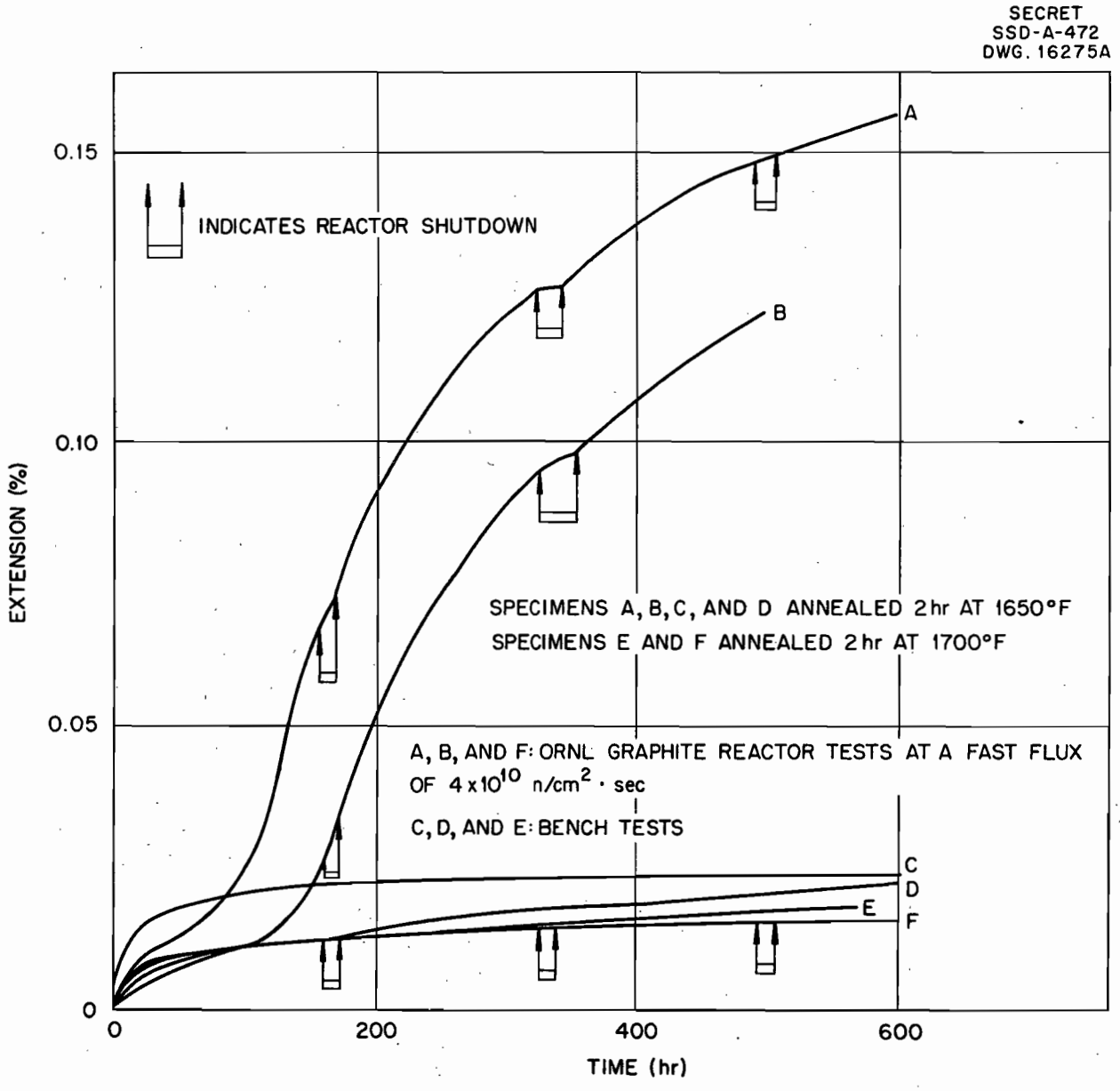

Fig. 1. Cantilever Creep Tests on Inconel at 1500°F and 1500 psi.

The sluggishness of the recrystallization process in Inconel is well known where only small amounts of cold reduction have preceded the anneal. Although the metallurgical history of the plate from which these specimens were made is unknown, hardness measurements indicate that it received about a 5% cold reduction after the penultimate anneal. Evidence of structural changes over long periods was found in the marked increase in intensity of all x-ray diffraction lines following a 1000-hr soak at 1500°F after the usual 2-hr anneal at 1700°F. Diffraction patterns of the outer fibers of both the compression and the tension sides of all the Inconel bench-test specimens have been made; more data are required for a detailed analysis, but it has been noted in all cases that the (111) line[1] is much more intense on the compression than on the tension side. No change in the

lattice constant of Inconel was found within the accuracy of measurement, approximately 1 part in 3000.

The strain-time curves for Inconel at 2000 psi and 1500°F after a 2-hr anneal at 1700°F are shown in Fig. 2. The in-pile curve was reported previously but the bench data were not complete at that time.[1] A test at 1000 psi was also run in the ORNL graphite reactor. It exhibited negative creep also, but not until after 200 hours. It reached a value of "negative strain" of nearly 0.1% after 400 hr and then proceeded normally at a rate one-half that of the 2000-psi test, also shown in Fig. 2. These results will be viewed skeptically until more tests are run. A LITR test at 2000 psi is now in its 400*th* hr; it shows less strain than the bench test of Fig. 2 at 400 hours.

Because of the behavior of the thermocouple circuit (described in next section "Effect of Radiation on Thermocouples") during the exposure of the initial two creep rigs in the LITR, the specimens were subjected to continuously increasing temperatures from the desired test temperature of 1500°F to between 1650 and 1700°F during a period of about 140 hr after the start of the tests. It is significant that the creep curves follow the bench tests fairly well until about 50 hr when the specimen temperatures certainly exceeded 1600°F. After this time, the creep rate begins to increase rapidly until at about 60 hr the range of the microformer was exceeded. The failure of irradiation

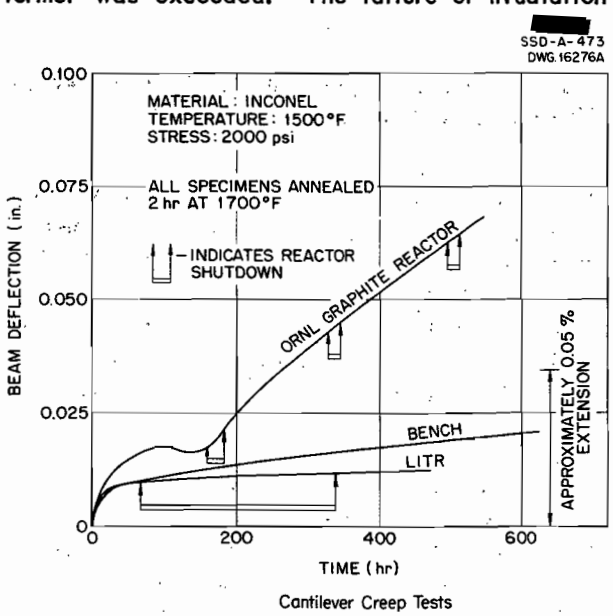

Fig. 2. Cantilever Creep Tests on Inconel at 1500°F and 2000 psi.

to produce appreciably more creep than in the bench tests until the test temperature was exceeded by over 100°F is a substantial qualitative indication of the creep resistance of Inconel under irradiation.

On the basis of three separate observations – the 1700°F-annealed specimen in Fig. 1, the 2000 psi LITR test mentioned, and deductions from the two LITR tests at 1500 psi – the creep strength of Inconel under irradiation at 1500°F appears to be of the same order as bench tests for a period of at least 50 hours.

EFFECT OF RADIATION ON THERMOCOUPLES

W. W. Davis J. C. Wilson
R. A. Weeks J. C. Zukas

After 10 hr of irradiation during the first LITR creep test it was observed that the power required to maintain the furnace at 1500°F continued to increase. A platinum resistance thermometer and a chromel-alumel thermocouple were built into a separate furnace alongside the second creep rig. In both tests the apparatus was in a helium atmosphere at a pressure of about 15 psi, and the thermocouple lead wire was a duplex, glass-insulated, 30-gage, chromel-alumel material manufactured by the Brown Instrument Company.

The second creep rig acted the same as the first in that it demanded ever-increasing power to maintain a constant thermocouple emf. The resistance thermometer and the thermocouple were intercalibrated in a narrow range at about 1500°F before the LITR came to power and at periodic intervals thereafter. The furnace power for a given reading of the resistance thermometer remained constant, whereas the emf of the thermocouple decreased with time. At 40 hr the output of the thermocouple indicated a temperature 100°F below that indicated by the platinum resistance thermometer. The leakage resistance between the two conductors of a duplex thermocouple lead wire, terminating in a ceramic insulator in the 1500°F zone, dropped continuously from 11 megohms to less than 0.7 megohm at the end of 145 hours.

A third rig was charged that contained another platinum resistance thermometer, several chromel-alumel thermocouples, and one platinum-rhodium thermocouple. Since it was suspected that the absence of air might have been responsible for the behavior of the earlier rigs, stagnant helium

was replaced with air flowing at a rate of 0.1 cfh for the first 65 hours. Based on the platinum-rhodium couple as a reference, the chromel-alumel couple changed 5°F during one week of irradiation, and the power input to the furnace remained constant during the test. The air was replaced with helium during the last 100 hr of the test. The helium produced only a slight shift in relative values of the readings because of its better cooling properties. The platinum resistance-thermometer readings decreased the equivalent of about 30°F during the test. The resistance thermometer in the second test was wound on alumina spacers; in the third test, it was wound in flexible fused-quartz sleeving. A bench test will be run on another thermometer in quartz sleeving to determine whether the output change was caused by contamination of the platinum by silicon.

From these tests it was concluded that the introduction of air into the apparatus eliminated the incorrect thermocouple readings that caused the failure of the first two creep tests. A 5°F difference in readings on the chromel-alumel and platinum-rhodium couples indicates little damage if it is assumed that there is small likelihood of both couples changing in exactly the same degree with respect to time. If the resistance thermometer is used as a reference, the couples change less than 30°F in the same period. This agreement is sufficient to assure fairly good data from Inconel tests at low stresses at 1500°F, pending more accurate thermocouple calibration with a melting-point apparatus.

The change of leakage resistance of the thermocouple wire is thought to be caused by the carbonization in inert atmospheres of the organic binder used in the fabrication of the deplex wire. The glass insulation, brown in color before the test, had a sooty appearance after heating to 1000°F in helium; the same treatment in air resulted in the insulation turning white. Apparently, in air, the products of the decomposition are carried off as gases. The convenience and space factor of the duplex lead dictate the continued use of this type of insulation if possible, and knowledge of its behavior in inert atmospheres as a function of temperature and irradiation is desirable.

The complexity and time-dependence of measurements of leakage resistance of the wire insulation may be seen in typical measurements in air and helium at different heating rates, as shown in Fig. 3. During the 29-hr test, the temperatures were

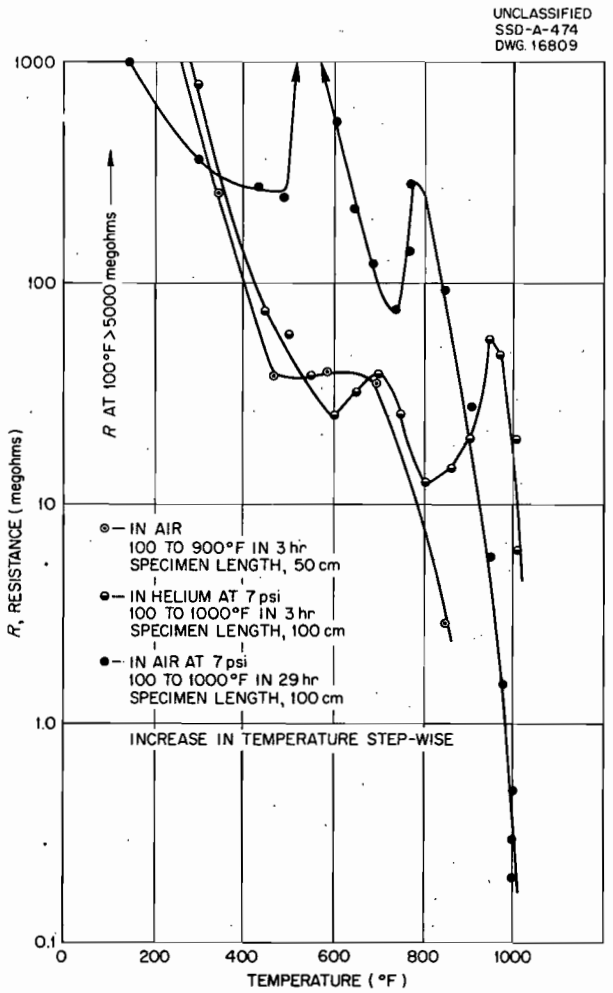

Fig. 3. Insulation Resistance of Chromel-Alumel Thermocouple Wire vs. Temperature.

varied in the following manner: from 100 to 500°F in 5 hr; 500°F for 16 hr during which the resistance increased to a value greater than 5000 megohms; and from 500 to 1000°F in 8 hours. The test section was a single-layer coil of the duplex wire that was wound on a $\frac{3}{8}$-in. mandrel. A test has been operating in helium at 700°F in a 540 r/min gamma source for 120 hr and the resistance has dropped from 300 to 15 megohms.

A miniature melting-point apparatus consisting of a sealed 1-in. length of $\frac{1}{8}$-in.-OD platinum tubing containing 0.1 g of sodium chloride has been operated. The difference between heating and cooling arrests at the melting point of the salt are, however, dependent on the rates of temperature change. By varying the furnace power input

slowly during heating and cooling, the rates can be preset and the disparity between the temperatures of the arrests decreased. A motor-driven variac to heat or cool at a given rate has been constructed.

Stability tests of 20-, 24-, and 30-gage chromel-alumel thermocouples have been made over 2000 hr at 1500°F in air. The indicated temperature deviation with time in Fig. 4 is referred to a platinum-rhodium couple that was inserted in the furnace a few hours before each reading and withdrawn immediately thereafter. The dips in the curves in the neighborhood of 33 hr and 55 to 60 hr are attributed to faulty placement of the calibrating couple. In all cases the emf indicated by the couples tends to increase with time at constant temperature.

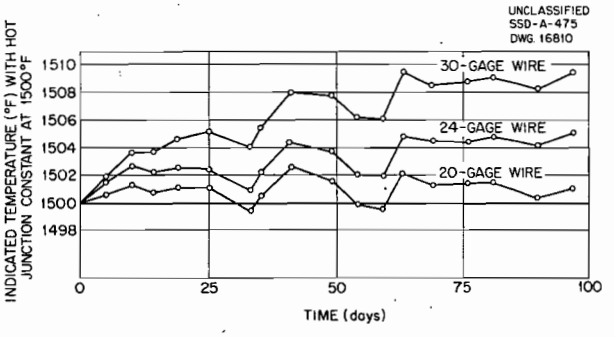

Fig. 4. Effect of Time on Readings of Chromel-Alumel Thermocouples in Air at 1500°F.

MTR CREEP EXPERIMENTS

J. C. Wilson

A bellows-loaded creep rig for the MTR has been designed and three units are being fabricated along with a bellows-calibrating device. The Instrument Department is conducting performance tests of several types of pressure-regulating valves to select the one giving best control for the bellows-pressurizing system. Design work on an alternate dead-weight-loaded apparatus is being initiated. A spring transducer[2] for test as an extensometer is also being built.

Delivery of the temperature controllers is scheduled for August. The experiment is scheduled for charging in the MTR on October 1. The safety circuits used in the LITR will be used with some modifications in the MTR.

[2] *Quar. Prog. Rep. of the Office of Basic Instrumentation Dec. 31, 1951*, p. 19, NBS-1467.

RADIATION EFFECT ON ELECTRONIC EQUIPMENT

R. A. Weeks

The irradiation of electronic equipment[1] was discontinued for the months of July and August because of other experiments scheduled for the bulk shielding facility. However, four units of electronic equipment (ARN-6, ARN-12, ARN-14, ARN-18) were each irradiated for over 100 hours. No change in their operating characteristics was observed. An interim report on the tests is now being written at Wright Field.

Measurements of the flux in the irradiation tank were made as follows: average fast neutrons, 2.5×10^7 neutrons/cm^2·sec; average thermal neutrons, 3×10^8 neutrons/cm^2·sec; and 4.8×10^9 one-Mev gammas/cm^2·sec. These values were somewhat lower than had been estimated from the data.[3] Irradiation of electronic units is scheduled to be resumed in September.

IMPACT TESTS ON IRRADIATED METALS

R. G. Berggren

Improvements on the remotely operated impact tester[4] are nearing completion. Modifications include hydraulic operation of the specimen vise, automatic specimen positioning, accommodation of cylindrical impact specimens up to 12 in. in length, facilities for cooling or heating the test specimen and vise, and a temperature-controlled pendulum trip. To save weight and space during irradiation, a subsize Izod specimen,[5] which consists of a series of notches 1 in. apart throughout the full length of the test specimens, has been adopted. The vise of the impact machine is deep enough to permit the unbroken section to extend below the machine. The specimen is then raised and positioned by remote control after each successive fracture. Trial runs of the machine have been made successfully at temperatures ranging from −190 to 80°C. Work is now being done to extend the upper limit of test temperatures to 200°C or higher.

[3] H. E. Hungerford, *Bulk Shielding Facility Water Data Work Sheet*, ORNL CF-52-2-37 (Feb. 1, 1952).

[4] W. Pate, E. Hutto, and E. Marguerat, *Nucleonics* 10, No. 6, 60 (1952).

[5] Specimen geometry originated by Argonne National Laboratory and shown on their Drawing No. NR-K-1852 A.

Impact tests on unirradiated titanium[6] (heat No. L782, alloy Ti 75A, Titanium Metals Corporation) have been initiated and specimens have been fractured at test temperatures ranging from 30 to −170°C. Tests at higher temperatures will be made when facilities for specimen heating are completed.

Impact specimens of normalized SAE 1040 steel have been irradiated in doughnut hole 1867 of the ORNL graphite reactor for periods of four and ten weeks (flux above 0.1 Mev equal to 8.3×10^{17} nvt and 3.0×10^{18} nvt, respectively) and in C-59 (vertical beryllium exposure piece) of the LITR for four weeks. The neutron spectrum in hole 1867 was measured and is reported in the "Neutron Measurements" section of this report. The flux in hole C-59 of the LITR will be monitored.

Impact specimens of type 304 ELC stainless steel are being irradiated in hole C-59 of the LITR; the duration of exposure is to be three months. Impact, tensile, and Young's modulus specimens of SAE 4340 steel and a tool steel[7] of various heat treatments have been prepared for irradiation in a Hanford-reactor process channel.[8]

[6] Work being done in collaboration with the Metallurgy Division.

[7] Analysis: 1.0% C, 1.2% Mn, 0.35% Si, 0.5% Cr, 0.5% W.

[8] In collaboration with R. H. Kernohan, Solid State Division, and with the Metallurgy Division. See "Special Projects" in Part II of this report.

ENGINEERING PROPERTIES

NEUTRON MEASUREMENTS

J. B. Trice

Neutron spectral measurements for future use in radiation-damage studies were completed in hole HB-2 of the LITR. Measurements in the low-energy region were made by using energy resonances in the cross sections for five (n,γ) nuclear reactions. These involved measuring the variation of cadmium ratios with distance from the blind (reactor) end of hole HB-2 for each reaction. The energy region covered in this manner extended from slightly above thermal energies up to about 10 kev. The spectrum above 0.6 Mev was measured by using threshold detectors.

Incidental to the measurements of spectra were measurements of the thermal neutron flux distributions for three reactor power levels: 850, 1000, and 1500 kw. Figure 5 shows the thermal-neutron flux traverses in hole HB-2. The 1500-kw traverse, which was extended 30 in. out from the active lattice, illustrates the rapidity with which the thermal flux decreases with distance.

The data necessary to determine the neutron energy spectrum in the kilovolt-energy region are summarized in Fig. 6, which shows cadmium ratios (ratio of activity of a material exposed directly to the flux to the activity of the material after exposure in cadmium) vs. distance from the active

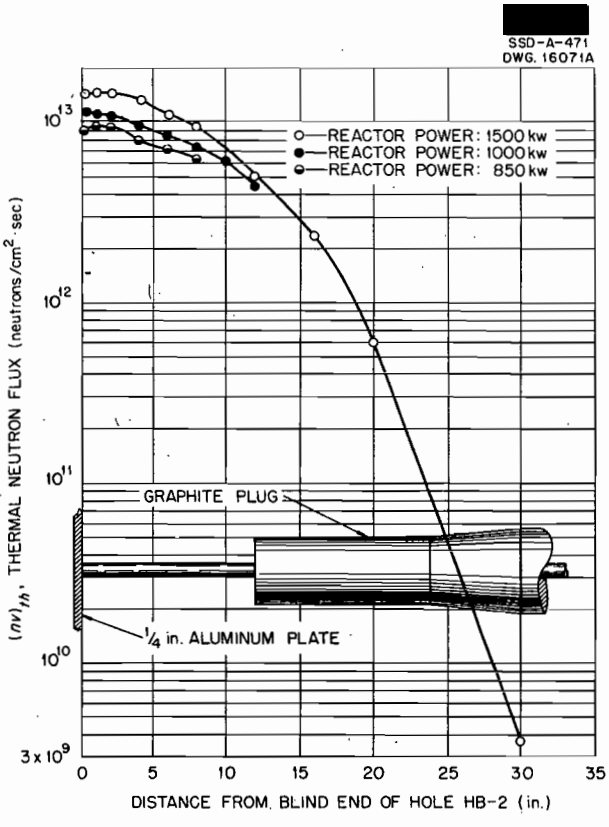

Fig. 5. Thermal-Neutron Traverses of Hole HB-2 for Three Power Levels.

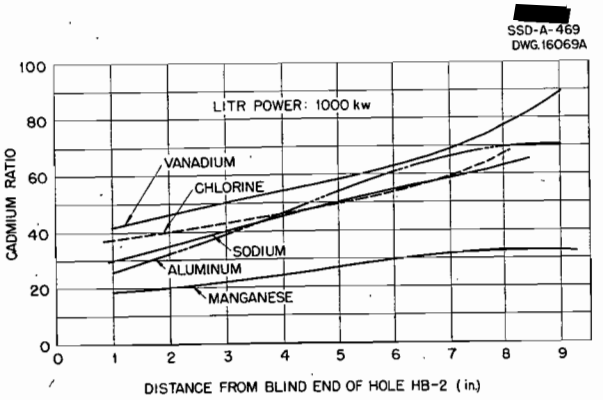

Fig. 6. Cadmium Ratios as a Function of Position in Hole HB-2.

lattice for five nuclear (n,γ) reactions. These reactions, which include energies from 261 to 9100 ev, result from irradiations of manganese, sodium, chlorine, vanadium, and aluminum. Activations that arise from cross-section absorption resonances determine cadmium ratios. These may then be used to determine whether the neutron energy distribution is inversely proportional to energy. The analytical procedure has been described.[1]

The constant ϕ_0 in the expression for the epithermal energy region of the spectrum,

$$\phi(E)\,dE = \frac{\phi_0\,dE}{E},$$

is determined from the equation

$$\phi_0 = \frac{\phi_{th}C}{(CR-1)(1+a)},$$

where C is a constant that corrects the thermal absorption cross section for the temperature and energy distribution of the reactor neutrons, a is an experimentally determined constant that refers to the resonance activation of the particular element used, and CR is the cadmium ratio. Values of ϕ_0 obtained from the five (n,γ) reactions had a small average spread of the order of 10 to 15% and were used to determine the best average value for ϕ_0, which is shown as a function of position in Fig. 7.

A summary of the data necessary to determine the spectrum in the energy region 0.5 to 7.0 Mev is shown in Fig. 8. Five threshold nuclear reactions are used here to determine the integrated spectrum above each energy threshold. These values for integrated flux are plotted as functions of position for each of the reactions. The data from these are then used to construct the curves shown in Figs. 8 and 9. Figure 9 shows integrated flux above threshold energy as a function of threshold energy, with the position in hole HB-2 as the varying parameter. Figures 10 and 11 show the neutron energy spectra in hole HB-2 from a perspective of two energy scales. The first of these, seen in Fig. 9, emphasizes the high-energy (0.6 to 7.0 Mev) region, whereas Fig. 10 gives a more complete picture of neutron spectra.

Figures 12, 13, and 14 show neutron spectral data for the ORNL graphite reactor doughnut hole 1867. These are similar to Figs. 9, 10, and 11

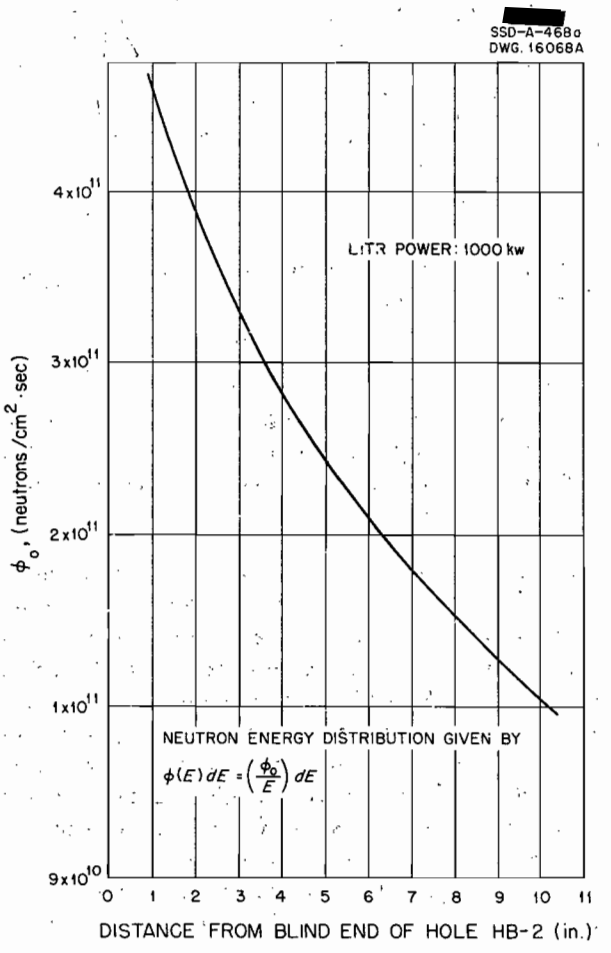

Fig. 7. Variation of ϕ_0 with Distance from End of Hole HB-2.

[1] S. M. Dancoff, H. V. Lichtenberger, R. G. Nobels, H. Kubitschek, and G. D. Monk, *Activation Cross Sections by Boron Absorption*, Argonne National Laboratory, CP-3781 (May 6, 1947).

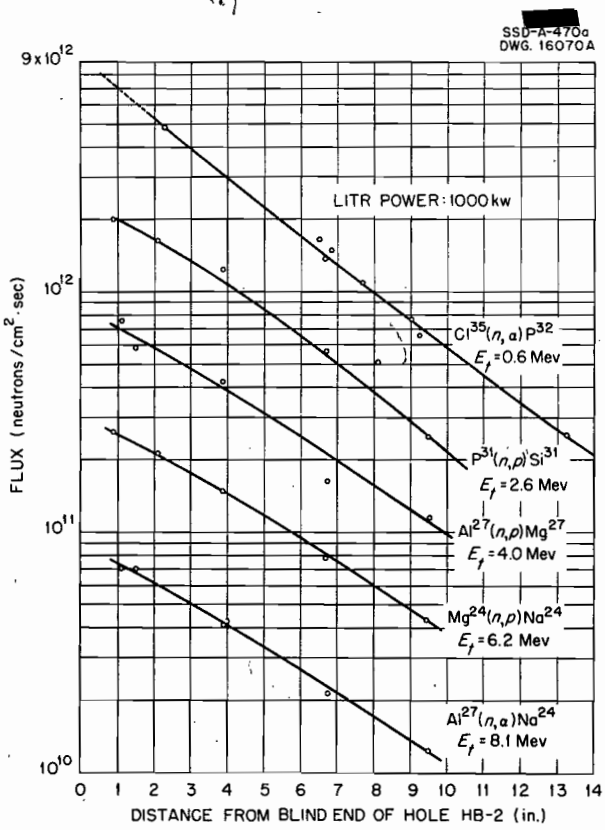

Fig. 8. Integrated Neutron Flux Above Nuclear Reaction Threshold Energies.

for the LITR. Figure 12 shows integrated neutron flux above threshold energies as a function of threshold energy. Figures 13 and 14 show the high-energy region and the complete neutron spectra, respectively.

In every case studied so far, the neutron spectrum, as measured in or near a strong moderating medium, consists of two well-defined energy regions. In one, a high-energy region that begins at approximately 0.5 Mev, the neutron spectrum strongly resembles the fission spectrum and above 3.5 Mev closely approximates the results reported by Watt.[2] From energies slightly above thermal up to the low-energy side of the fission spectrum the neutron energy distribution appears to obey a dE/E law. Ideally, in the case of very good moderation, these two regions should join each

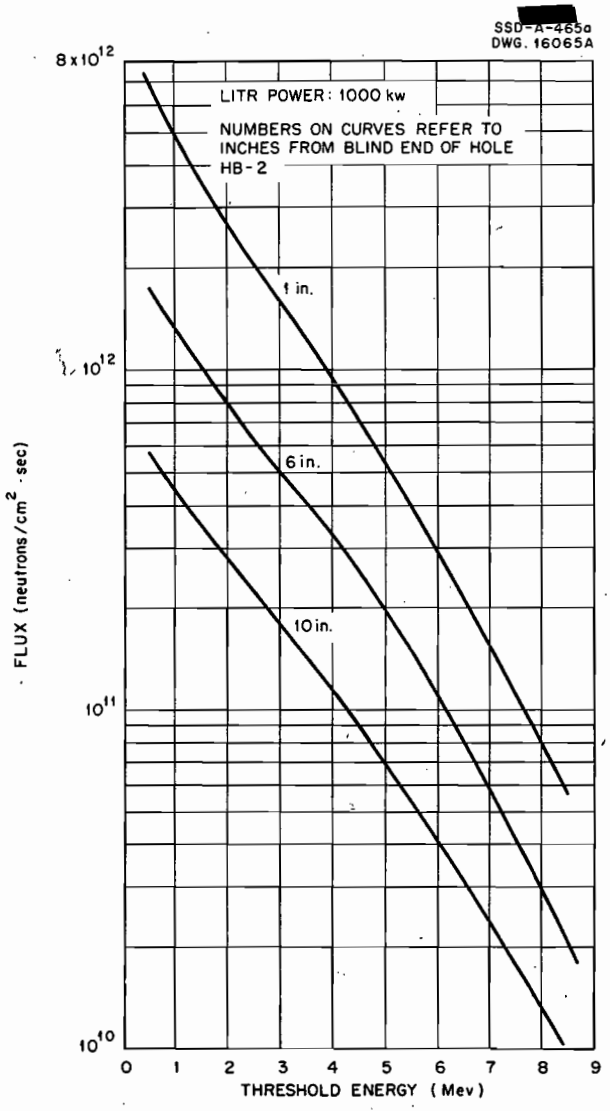

Fig. 9. Integrated Neutron Flux Above Threshold Energies as a Function of Threshold Energy.

other smoothly at the low-energy side of the fission spectrum. However, where moderation is poor, the high-energy region shows up prominently, following closely the fission spectrum as the moderation decreases. This can be illustrated by the cases described. In hole HB-2 the relative number of neutrons in a given energy band shifts toward lesser energy values with increasing (more moderation) distance from uranium metal. Also, in the case of hole 1867, the fission region is very prominent because the hole passes directly through the fissioning material.

[2] B. E. Watt, *Energy Spectrum of Neutrons from Fissions Induced by Thermal Neutrons*, LA-718 (Dec. 17, 1948).

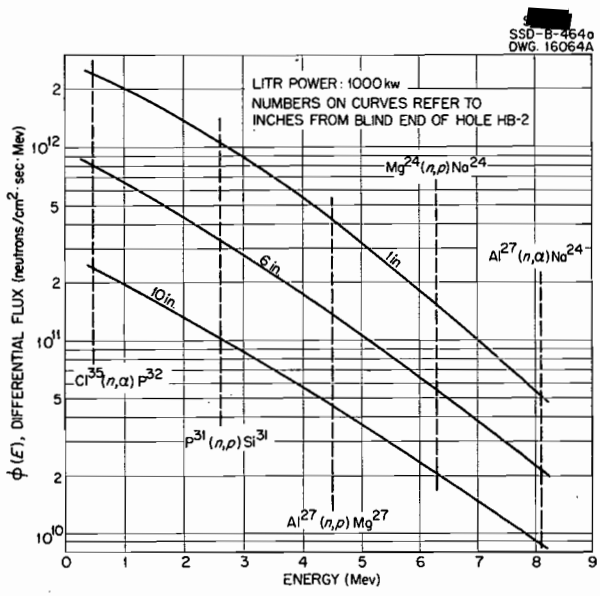

Fig. 10. High-Energy Neutron Spectra at Various Locations in Hole HB-2.

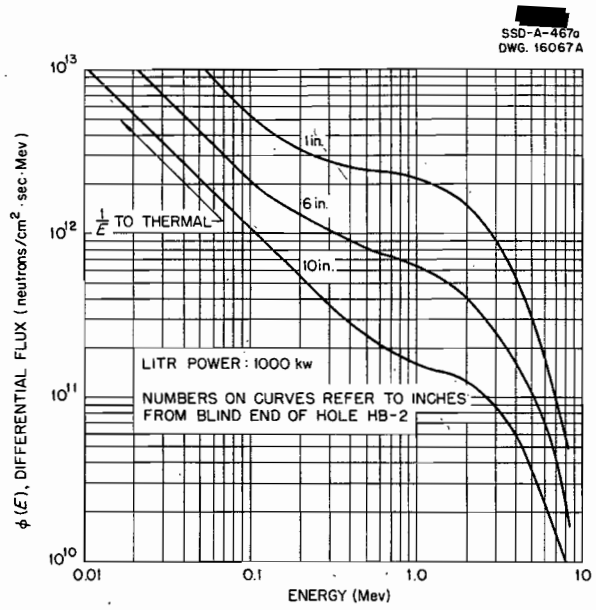

Fig. 11. Total Neutron Spectra at Various Locations in Hole HB-2.

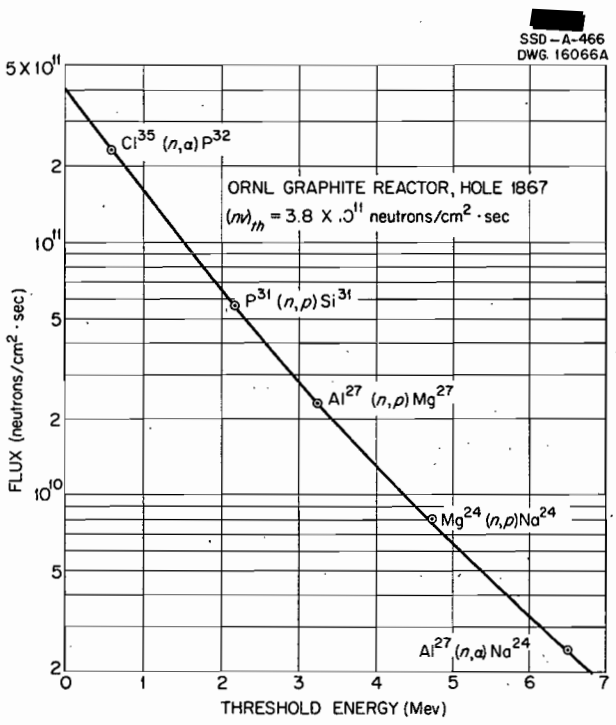

Fig. 12. Integrated Neutron Flux Above Threshold Energy as a Function of Threshold Energy.

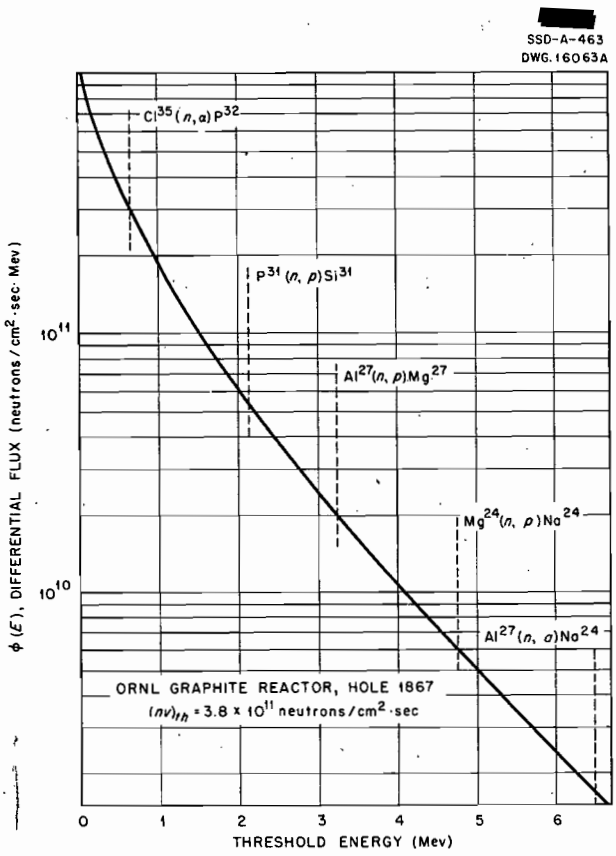

Fig. 13. High-Energy Neutron Spectrum.

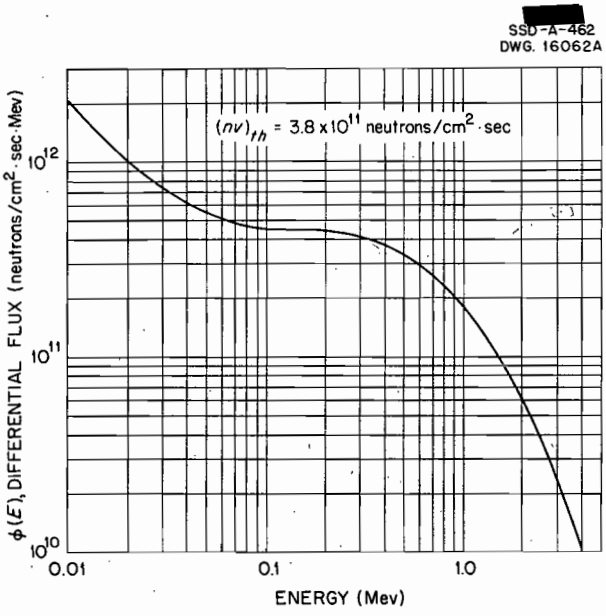

Fig. 14. Total Neutron Spectrum in ORNL Graphite Reactor Hole 1867.

NUCLEAR-REACTION STUDIES

J. B. Trice

It is possible to calculate the threshold reaction energies by using the values reported in the literature for the isotopic masses. In the case of $Cl^{35}(n,\alpha)P^{32}$, the isotopic mass of P^{32} is not known well enough to permit an accurate estimate of the threshold. Some values given indicate the reaction to be exoergic with about a ½-Mev excess binding energy;[3] other values show it to be endoergic with a threshold at about 0.6 Mev.[4] The cadmium ratio for this reaction, measured in hole 1867 of the graphite reactor, was unity. This indicates that the reaction is endoergic, since it shows that thermal neutrons cause no activation. If a reported value of 0.017 barn given for the cross section at ~3 Mev[5] is used and if it is assumed that the cross section for the $Cl^{35}(n,\alpha)P^{32}$ reaction behaves in a manner similar to the $P^{31}(n,p)Si^{31}$[6] and the $S^{32}(n,p)P^{32}$[7] reactions, it appears that the effective threshold energy occurs at approximately 0.6 Mev for reactor-type neutron spectra. More complete confidence can be placed in this reaction when the cross section is known as a function of energy.

The $N^{14}(n,p)C^{14}$ nuclear reaction was used as a partial check on the neutron spectrum in the LITR, hole HR-1, measured by the methods described above, and reported in the last quarterly report.[8] The experimentally determined function was used together with the (n,p) cross section as a function of energy to estimate the C^{14} activity produced from 2.3 g of Be_3N_2 irradiated for 591.7 hr at an average operating power level of 983.2 kilowatts. The experimental analysis of the Be_3N_2 sample, performed by R. P. Shields and E. I. Wyatt of the ORNL Operations Division, yielded 1.5 μc of C^{14}. This was considered excellent agreement since the principal activation of the reaction occurs in the energy region 0.5 to 1.5 Mev, which is the spectral region of most uncertainty.

ORNL GRAPHITE REACTOR LIQUID-METALS LOOP

C. D. Baumann, C. Ellis, F. M. Blacksher, M. T. Morgan, R. M. Carroll, O. Sisman, W. W. Parkinson

For some time a program has been under way to investigate the compatibility of various high-temperature coolants and structural materials under reactor irradiation. Dynamic systems made of loops of Inconel tubing circulating rhodium are being tested in the ORNL graphite reactor.

The loop that had developed a plug after two weeks of operation[8] was found to have an obstruction composed of fine, powdery material. This material was analyzed spectrographically, and it contained much less chromium, somewhat less iron, and appreciably more nickel than normal Inconel. The other constituents of Inconel were found in approximately correct amounts. Since the sample was found in the cool zone, the disproportionate amounts of nickel and chromium may

(3) J. Mattauch and A. Flammersfeld, *Isotopic Report*, Verlag Der Zeitschrift Fur Naturforschung, Tubingen, 1949.

(4) C. D. Hodgman (ed. in chief), *Handbook of Chemistry and Physics*, 32d ed., Chemical Rubber, Cleveland, 1950-51.

(5) *Metallurgical Laboratory, Argonne Laboratory Division, Report for April, May and June, 1946*, CF-3574.

(6) E. Bretscher and D. H. Wilkinson, *Proc. Cambridge Phil. Soc.* 45, 141 (1949).

(7) E. D. Klema and A. O. Hanson, *Phys. Rev.* 73, 106 (1948).

(8) *Solid State Quar. Prog. Rep. May 10, 1952*, ORNL-1301 (in press).

be due to mass transfer wherein material that went into solution in the hot zones of the loop was partially precipitated in cooler zones. Alternately, the material may be the insoluble metallic residue from the reaction of sodium with oxides of nickel, chromium, iron, etc. that might have been present as surface oxides and welding scale.

Metallographic examination of the specimens cut from the exterior and in-pile portions of the loop has been completed, and, in addition, an examination has been made of pieces cut from the "as-received" tubing used to fabricate the loop. The latter pieces were used as control specimens, and photomicrographs of them are shown in Fig. 15*a* and c. Figure 15*b* shows the specimen cut from the unirradiated portion of the loop that was at about 1000°F during the 120 hr of operation. Figure 15*a* shows the control from the same length of tubing as this unirradiated specimen, whereas Fig. 15c presents the control from the tubing for the irradiated specimen, Fig. 15*d*. The irradiated part of the loop operated at about 1500°F during the approximately 120-hr exposure in the reactor. The grain size and surface condition of the two treated specimens compare quite similarly with the respective controls, but a precipitate has appeared in the grain boundaries of the unirradiated specimen, Fig. 15*b*. The precipitate is probably a carbide, and its presence in the unirradiated specimen and absence in the irradiated specimen may be due to the difference in composition of the two lengths of tubing used for these portions of the loop, although both were received on the same purchase order. It is more likely that the difference in operating temperatures of the two portions of the loop was responsible for the precipitate in one case and its absence in the other. To investigate this possibility, portions of the two controls are being heat-treated at the two temperatures, 1000 and 1500°F. It is not considered probable that neutron bombardment prevented the precipitation in the irradiated specimen. The exposure to flowing sodium apparently had little effect on the Inconel since the surfaces of the exposed specimens are very similar to the surfaces of the unexposed controls. Finally, there was no appreciable reduction in wall thickness of the tubing that contained the circulating sodium.

Two new loop assemblies of Inconel tubing have been built with by-pass circuits in the out-of-pile sections. The by-pass circuit contained a settling and cooling tank and a micrometallic sintered stainless steel filter to remove oxides or other solids from the sodium. These loops were filled with sodium and bench tested, but each developed a leak despite the rigorous inspection and leak-testing procedure described in the previous report.[8] In both cases the leaks developed at the junction of a tube and the in-pile end block or U turn. Examination of the welds indicated that the leaks developed at the point where the weld bead overlapped the starting point of the weld. The Metallurgy Division suggests that the leaks were caused by surface oxides at the start of the weld being covered by the overlap at the end of the weld. To eliminate the possibility of this recurring, the next weld will be backed with a nickel-palladium braze.

To measure the activity of liquid metal circulating through the loop in the reactor, an ionization chamber is located beneath a hole in the lead shield under part of the loop outside the reactor. The efficiency of this chamber is being calibrated to provide an absolute measurement of the radioactivity of the metal stream and for earlier measurements of bremsstrahlung associated with circulating lithium.[9] The chamber was initially calibrated with Co^{60} samples (average photon energy, 1.25 Mev), but since the efficiency of an ionization chamber varies with the energy of the incident radiation, a mockup of the experimental arrangement is being calibrated with gamma radiation of various energies. Co^{60}, Cs^{137}, Cr^{51}, Hg^{203}, and Ti^{204} were used as sources because they give gamma radiation that is monoenergetic, or nearly so. These materials cover a wide range of energies. The initial measurements indicate that the efficiency for low-energy photons is less than that of a "100% geometry" chamber and is slightly less than would be obtained assuming linear dependence of efficiency upon energy.

STANDARDIZATION OF LIQUID-METAL FLOWMETERS[10]

R. M. Carroll

In an effort to eliminate the frequent breakdowns and uncertainties that have been experienced in the operation of electromagnetic flowmeters, a

[9] C. D. Baumann, R. M. Carroll, O. Sisman, W. W. Parkinson, and C. Ellis, *Solid State Quar. Prog. Rep. Oct. 31, 1951*, ORNL-1214, p. 35.

[10] Topical report being prepared.

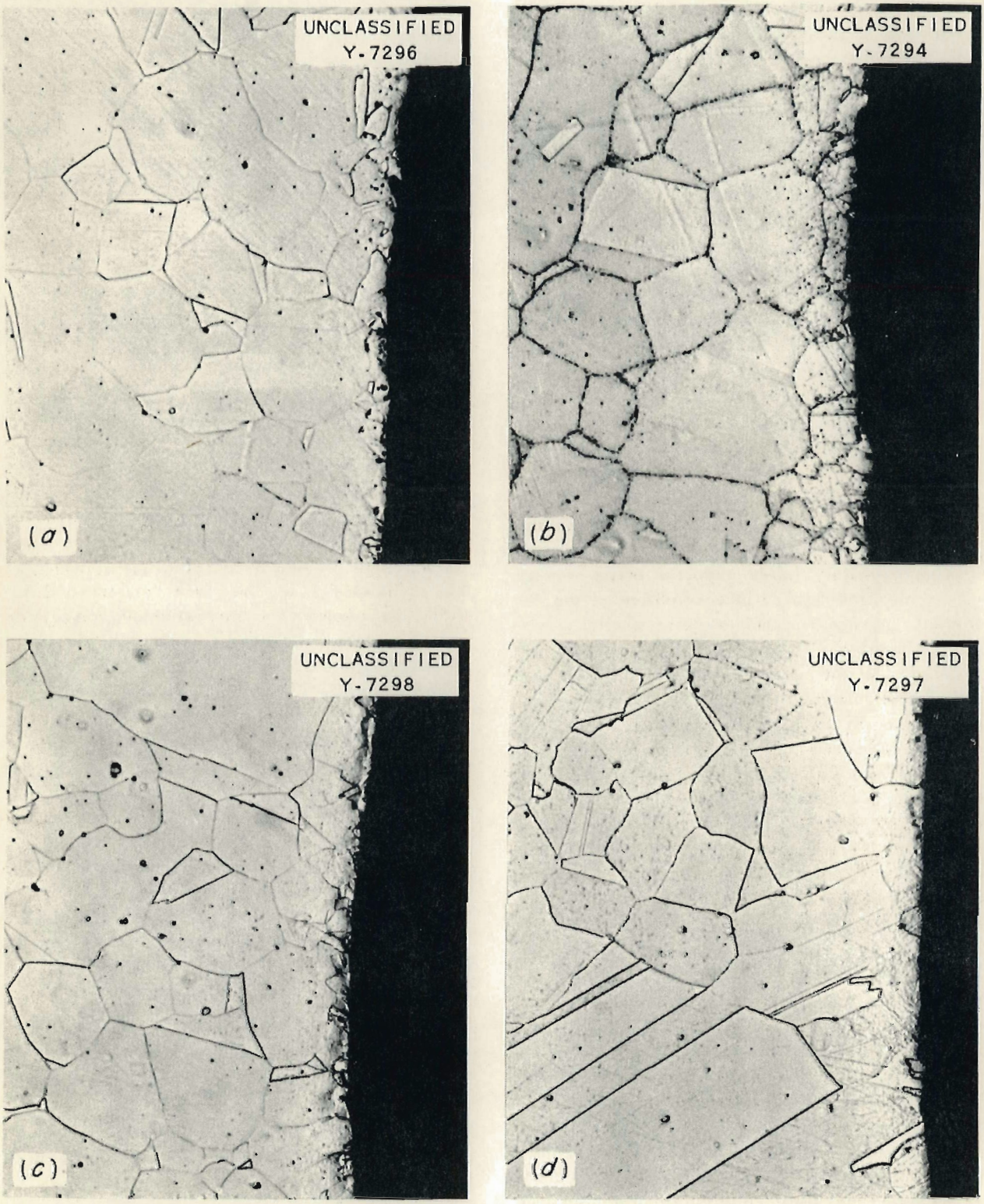

Fig. 15. Inconel Corrosion Specimens. (*a*) Control specimen, as-received tubing. (*b*) Specimen cut from unirradiated portion of loop. (*c*) Control specimen, tubing used for irradiated specimen. (*d*) Irradiated specimen.

UNCLASSIFIED
PHOTO 10113

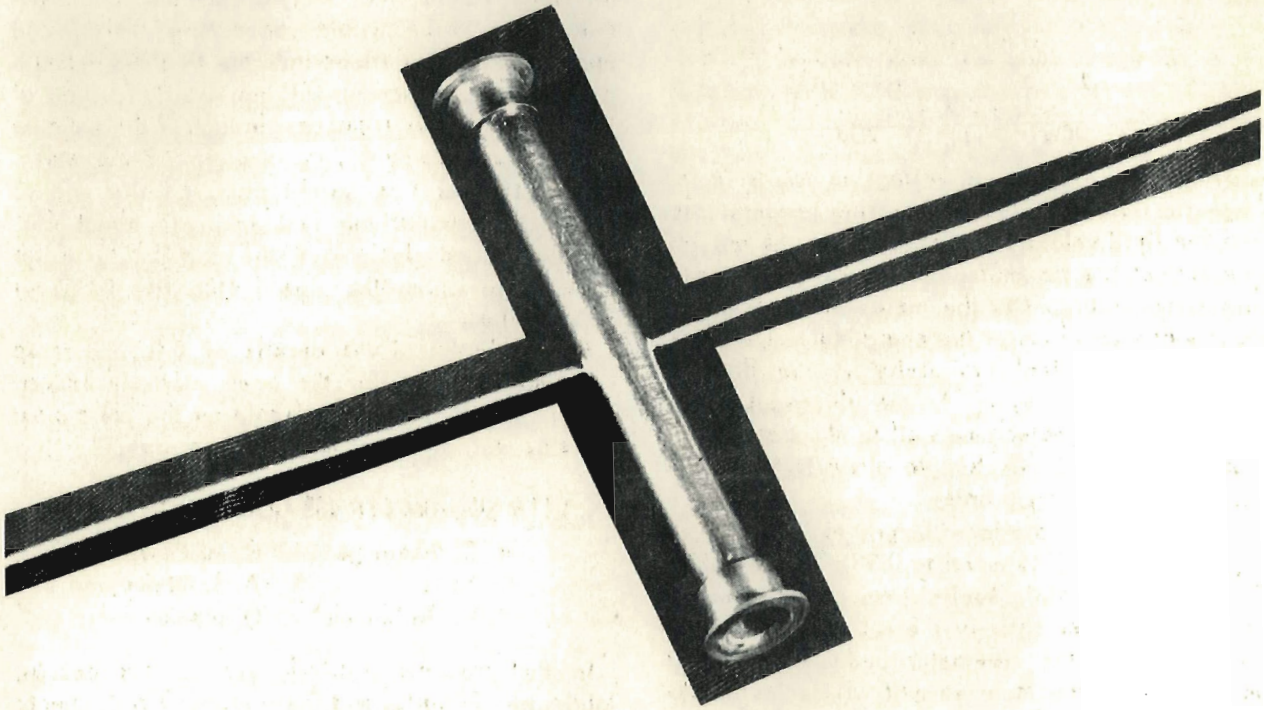

Fig. 16. Liquid Metal Flowmeter.

standard type of flowmeter has been designed and several have been built of Inconel and stainless steel in various sizes (Fig. 16 is typical). These have been connected into a sodium-tank system for calibration, as described earlier.[8] The cells were calibrated by passing measured volumes of sodium through them at a rate that generated a given emf and then measuring the time required for passage of the sodium. This method of calibration was accurate enough to give experimental points within ±0.5% of a straight line. A typical calibration curve is shown in Fig. 17 and it was found that duplicate cells, of the same size and material, differed by not more than 1% in calibration. This was also the limit of variation between cells of the same size but made of Inconel and type 316 stainless steel.

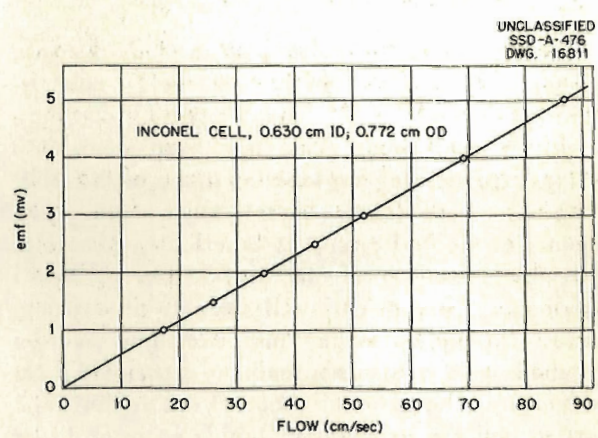

Fig. 17. Typical Flowmeter Calibration Curve.

The potential developed for various flow rates, flowmeter sizes, and materials of construction was predicted to within 3% by the theoretical formula[11] for a flowmeter with a conducting tube wall:

$$E = \frac{(Bdv)\,(K) \times 10^{-5}}{\dfrac{D^2 + d^2}{2Dd} + \dfrac{\rho_f}{\rho_w}\left(\dfrac{D^2 - d^2}{2Dd}\right)},$$

where E is the generated voltage in mv, B is the magnetic field in gauss at operating temperatures, v is the fluid velocity in cm/sec, D is the outside diameter of the flowmeter tube in cm at the operating temperature, d is the inside diameter of the flowmeter tube in cm at the operating temperature, ρ_f is the electrical resistivity of the fluid in ohms at temperature, ρ_w is the electrical resistivity of the flowmeter-tube wall in ohms at temperature, and K is a constant to allow for the magnetic field not being infinite.

For ratios of pole-face length to diameter of approximately 3, K is equal to 0.98. The deviation of the experimental results from the theoretical formula is almost entirely the result of the small dimensions of the flowmeter and the attendant uncertainty of the measurement of its inside diameter; that is, the inside diameter of a tube nominally 0.125 in. may be difficult to determine to less than ±0.002 inch. If greater accuracy and uniformity are desired, the flowmeter tubes should be precision bored so as to have uniform roundness and wall thickness.

MTR FLUORIDE-FUEL LOOP

W. W. Parkinson O. Sisman

An apparatus is being designed to study dynamic corrosion of Inconel by fluoride fuels under irradiation in the MTR.[8] The design of a compact, air-driven centrifugal pump has been completed by the Experimental Engineering group of the ANP Division. The design of the other major components of the fuel circuit is practically complete, with the exception of the preparation of detail drawings. This circuit will consist of a pump, venturi flowmeter, surge tank, irradiated section attached to a heat sink, and an air-cooled heat exchanger. The external shape of the venturi tube section and the associated liquid-separator tanks and pressure-measuring system have been designed. Design is also complete for the surge tank, the U-shaped test section and its heat sink, and the heat exchanger. The pressure drop for the air required by the heat exchanger has been calculated to be within reasonable limits, and approximate calculations indicate that the exhaust air from the exchanger will not melt the lead of the shield plug as it passes through if the exhaust line is insulated by $^7/_{16}$ in. of diatomaceous earth. The design of this shield plug, on the end of which is mounted the fuel loop, is about 70% complete, and design of the full-length water jacket into which the shield plug fits is about 30% finished.

A description of the details of this apparatus is being reserved for the next quarterly report. Drawings will then be available on the component parts as well as the assembled apparatus.

LITR SODIUM STRESS-CORROSION LOOP

W. E. Brundage R. M. Carroll
C. Ellis A. S. Olson
W. W. Parkinson O. Sisman

In the previous quarterly reports the design, fabrication of parts, and the testing of components for an apparatus for circulating molten sodium through a stress-corrosion specimen in the LITR were described. At the present time the design is complete and fabrication of parts of the loop is about 98% complete; the apparatus is about 70% assembled.

Supports for the external section of the loop and its shielding are about 10% complete. The outer plug and water jacket are being rebuilt after it proved impossible to install them because of distortion in hole HB-2. The original plug was turned down in an effort to reduce its size sufficiently to fit the hole, but several attempts at installation failed. The distortion seems to lie in the center of the nominal 7-in. section of the hole. The Reactor Operations Department recommended that this section of the plug be omitted or made as small as possible. The minimum dimensions that could be used for the experiment were determined and a wooden plug was turned from a section of a telephone pole to these dimensions. This plug went into the hole easily and the dimensions of this mockup plug will be used as the maximum dimensions for the new plug that is being

[11] E. R. Astley, *Magnetic Flowmeter Output Potentials*, R52GL42 (March 1, 1952).

fabricated. The aluminum water jacket on the inner end of the original plug was salvaged and will be used on the new plug.

The stress-corrosion specimen was checked by x ray and it was found that the axially-mounted, $^1/_8$-in., filler rod used to increase the fluid velocity through the specimen had sagged and was touching the wall of the specimen. The specimen also had a chip of foreign material in it. The end of the specimen was machined off to permit removal of the rod. A new filler rod was made from a uranium–stainless steel sandwich tube furnished by the Metallurgy Division in the hopes of obtaining some data on a fuel-bearing assembly. The sandwich tube (the filler rod) was sealed at each end with a plug. One plug had small pins projecting radially from it to support the end of the rod, which was formerly unsupported. The other end cap fitted the hole that had been machined in the end of the specimen to remove the sagging rod. These filler rod components were nickel-palladium brazed and then welded into the specimen. Welding was used rather than brazing to avoid the possibility of sagging the filler rod again.

FUSED SALTS

ZIRCONIUM-BASE EUTECTIC SALTS

G. W. Keilholtz M. J. Feldman
P. R. Klein C. C. Webster

The zirconium-base salt, reactor fuel No. 21, has been irradiated at 140 w/cc in the LITR. No pressure effects have been noted. The metallurgical examination of irradiated samples is in process. Chemical analyses of the first series of samples do not show any serious radiation damage effects. It appears at this stage that zirconium-base eutectic salts are comparable in radiation stability to beryllium-base eutectic salts.

LIQUID-FUELS IRRADIATION IN THE MTR

J. G. Morgan H. E. Robertson
A. E. Richt

The equipment for irradiation of liquid fuels has been shipped to the MTR at Arco and final installation is now in process at the site. This equipment will be used to study radiation stability of ANP liquid fuels at 3000 w/cc, or at a thermal flux in the range of 4×10^{14}.

XENON-135 IN FLUORIDE FUELS

M. T. Robinson D. D. Davies

An experiment has been performed to determine the fate of Xe^{135} produced by fission in the fused-fluoride aircraft reactor fuels. Two runs were made under identical conditions, except that in the first run xenon was flushed out by bubbling helium carrier gas through the melt, whereas in the second run carrier gas merely swept over the surface.

The helium carrier gas was of the best grade obtainable and was further purified by passing over hot copper and dried over anhydrous magnesium perchlorate. The gas was conducted to the fuel-containing capsule, suspended in hole 12 of the ORNL graphite reactor, through 30 ft of 0.036-in. stainless steel capillary tubing. After passing through the capsule, the gas was carried by a similar length of tubing to a trap cooled by a dry ice–acetone mixture where volatile materials were removed, to a charcoal trap, also cooled by dry ice–acetone, for removal of xenon, and finally, through a flowmeter, to the reactor off-gas system. The flowmeter was designed and constructed by J. N. Baird, Jr., of the ORNL instrument department and has a range of about 10 to 60 ml (STP) of helium per minute. A flow rate of 15 ml/min was used for these experiments.

The fuel capsule used in the flushing experiment is shown in Fig. 18. The carrier gas was led in through the small hole to the cavity at the bottom of the capsule; it then passed through the sintered-steel plate, bubbled through the melt, and left the capsule at the top. The capsule for the sweeping experiment had exactly the same geometry, except that the porous plate was not present and the gas inlet entered directly into the fuel chamber.

The fuel sample in each case was 1 g of normal No. 2 fluoride fuel[1] containing 3.79 mg of U^{235}. It was irradiated at a thermal flux of 7×10^{11} neutrons/cm^2·sec for 31 min. After waiting 4.5 hr for short-lived activities to decay, helium flow was

[1] 27.5 mole % UF_4, 46.5 mole % NaF, 26.0 mole % KF, m.p. 530°C.

TABLE 1. RESULTS OF XENON-135 EXPERIMENT

	INTEGRATED FLUX (Al-Mn-Co Monitor) (v/mg)	Xe^{135} FOUND (v)	Xe^{135} EXPECTED (v)
Flushing	0.117	1.44	
Sweeping	0.097	0.032	1.22

started and continued until 11 hr had elapsed from the end of the irradiation. The sample was maintained at 650 to 750°C throughout the experiment.

The thermal-neutron dose was monitored with a clip of Al-Mn-Co alloy that was removed immediately after the irradiation was completed. The amount of Xe^{135} was determined by transferring the contents of the charcoal trap to a counting vessel and counting in a 4π-geometry high-pressure chamber. All counting and trap preparation was carried out by W. A. Brooksbank of the Analytical Chemistry Division. The results of the experiments are recorded in Table 1. The integrated fluxes and the amounts of Xe^{135} found are reported in terms of the response of the particular counter employed. No absolute calibration was made. On the basis of the different flux in the sweeping experiment (in which about 5% more U^{235} was present), the expected Xe^{135} value was calculated from the result obtained in the flushing run. Only about 2.5% of the expected Xe^{135} was obtained.

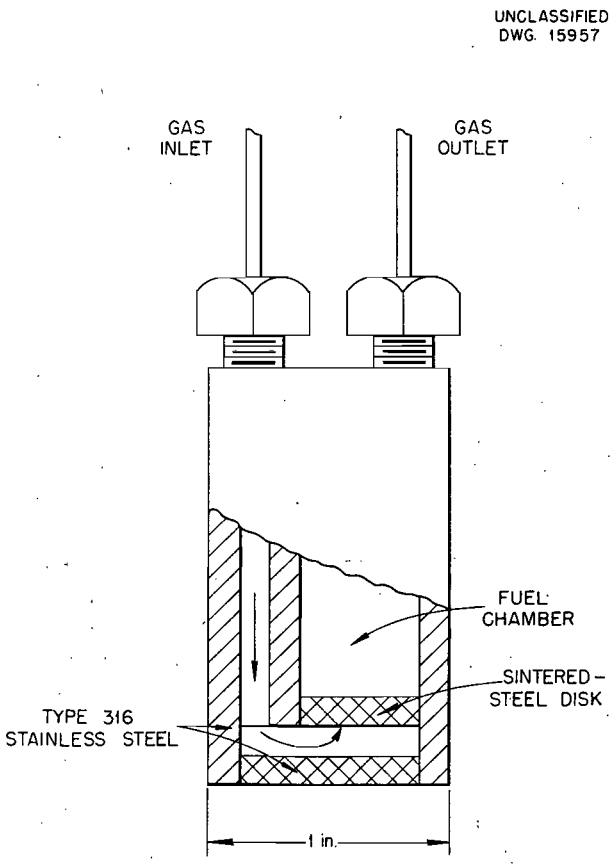

Fig. 18. Gas Flushing Capsule.

The following conclusions can be drawn from these results: (1) Fission-produced iodine (e.g., I^{135}) does not appear in the fluoride melt in a volatile form such as IF_5 or I_2. If such species had been present, Xe^{135} would have been observed in larger amounts in the sweeping experiment. Iodine probably occurs as the simple iodide ion, I^-. (2) It appears probable that Xe^{135} diffuses slowly in the fluoride melt. The Mathematics Panel has agreed to obtain appropriate numerical solutions to Fick's differential equation by using diffusion coefficients calculated from the Einstein-Stokes equation (for the liquid phase) and elementary kinetic theory of gases (for the vapor phase). The results of the computations will provide a theoretical check on the experimental results.

RADIATION STABILITY OF COPPER PHTHALOCYANINE

M. T. Robinson G. E. Klein

Although organic compounds are generally considered to be too unstable to permit reactor applications, the work of Sisman and Bopp[2] on irradiation of plastics indicates wide variations in

[2] O. Sisman and C. D. Bopp, *Physical Properties of Irradiated Plastics*, ORNL-928 (June 29, 1951).

the resistance of such materials to decomposition in the presence of ionizing radiation. Perhaps one of the most stable organic substances at elevated temperatures is the brilliant-blue pigment, copper phthalocyanine ($C_{32}H_{16}N_8Cu$), called "Solfast Sky Blue."[3]

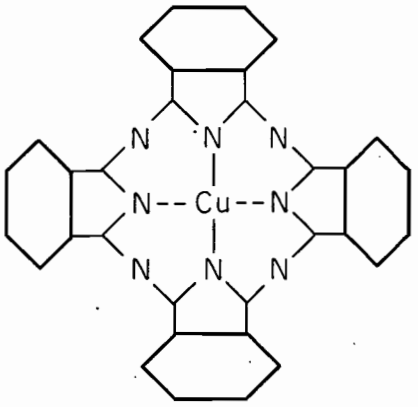

Preliminary experiments conducted over the past year indicate a surprising degree of chemical stability, but x-ray diffraction patterns showed a number of interesting changes. Exposures to a flux of 5×10^{11} neutrons/cm^2·sec for periods up to 209 days failed to produce any detectable chemical destruction of the compound.

A large batch of the material has been obtained and was shown by x-ray diffraction to be the unstable alpha modification.[4] The pattern has been indexed as tetragonal crystals with lattice constants $a_0 = 17.1$ Å and $c_0 = 12.8$ Å. The unit cell volume is 3755 Å^3. The density has been found to be 1.53 g/cc by water displacement. Hence, there are 6 molecules per unit cell. The probable space groups (among which no choice can presently be made) are D_{4h}^{14} – *P4/mnm*, D_{4h}^{7} – *P4/nmm*, D_{4h}^{1} – *P4/mmm*, and C_{4h}^{3} – *P4/n*. The last group seems least likely because of the difficulty of placing all atoms in acceptable positions.

A small quantity of the stable beta modification of the pigment has been prepared by mulling the alpha form in cyclohexanol. X-ray diffraction patterns are substantially identical to that reported by Robertson.[5] It is a monoclinic crystal of space group C_{2h}^{5} – *P21/a*, containing 2 molecules in a unit cell of 1180 Å^3 volume.

[3] Sherwin Williams Co. trademark for copper phthalocyanine.

[4] D. P. Graham, U. S. Pat. 2,556,730 (June 12, 1951).

[5] J. M. Robertson, *J. Chem. Soc.* p. 615-621 (1943).

IRRADIATION FACILITY IN HOLE HB-6 OF THE LITR

M. T. Robinson B. W. Kinyon

A facility has recently been installed in hole HB-6 of the LITR that will allow exposure of small samples (fused salts, organic materials, etc.) for periods of weeks. Only a small portion of the plug need be removed from the reactor when changing samples. The irradiated specimens are air-cooled to prevent overheating the plug. Instrumentation to control and to measure specimen temperatures is substantially complete and will be installed shortly. A drawing of the facility is shown in Fig. 19.

DYNAMIC RADIATION-DAMAGE STUDIES

D. F. Weekes J. G. Morgan
P. R. Klein H. E. Robertson
A. E. Richt

All radiation-damage studies have been made in static capsule tests. Since ARE fuels will be used in flowing systems in and out of high neutron flux, an assembly has been made to simulate these conditions.

In the dynamic corrosion test to be conducted in hole HB-2 of the LITR, an Inconel capsule containing a small volume of liquid fuel will oscillate with an amplitude of 20 deg about a horizontal transverse axis to permit the fuel to flow back and forth over the wall of the capsule as shown in Fig. 20. At one end of the capsule, the fuel will be maintained at 800°C by a coaxial heater and will be exposed to practically the full thermal-neutron field of the reactor. At the other end, the fuel will be shielded from thermal neutrons by surrounding the end of the capsule with a coaxial, absorbing cylinder of Boral. Space limitations and the thermal properties of Boral determine the length and diameter of this cylinder. To estimate its effectiveness as a shield, it is necessary to compare the flux at the center, arising from entry of thermal neutrons at the ends, with the flux at the exposed end of the capsule.

Let Σ_s, Σ_t, and ϕ be scalar-point functions representing the macroscopic scattering and total cross sections of a medium for thermal neutrons

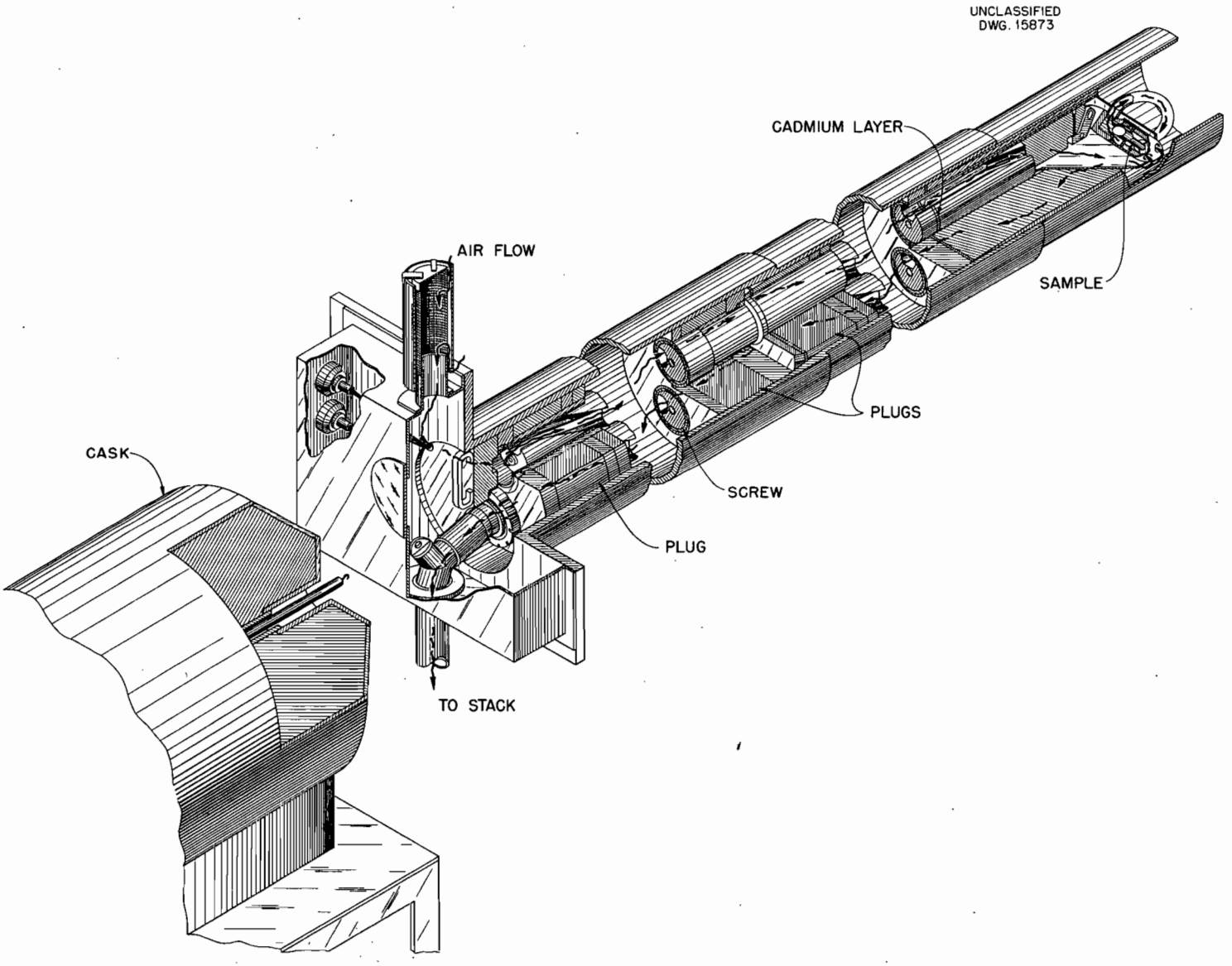

Fig. 19. LITR HB-6 Installation.

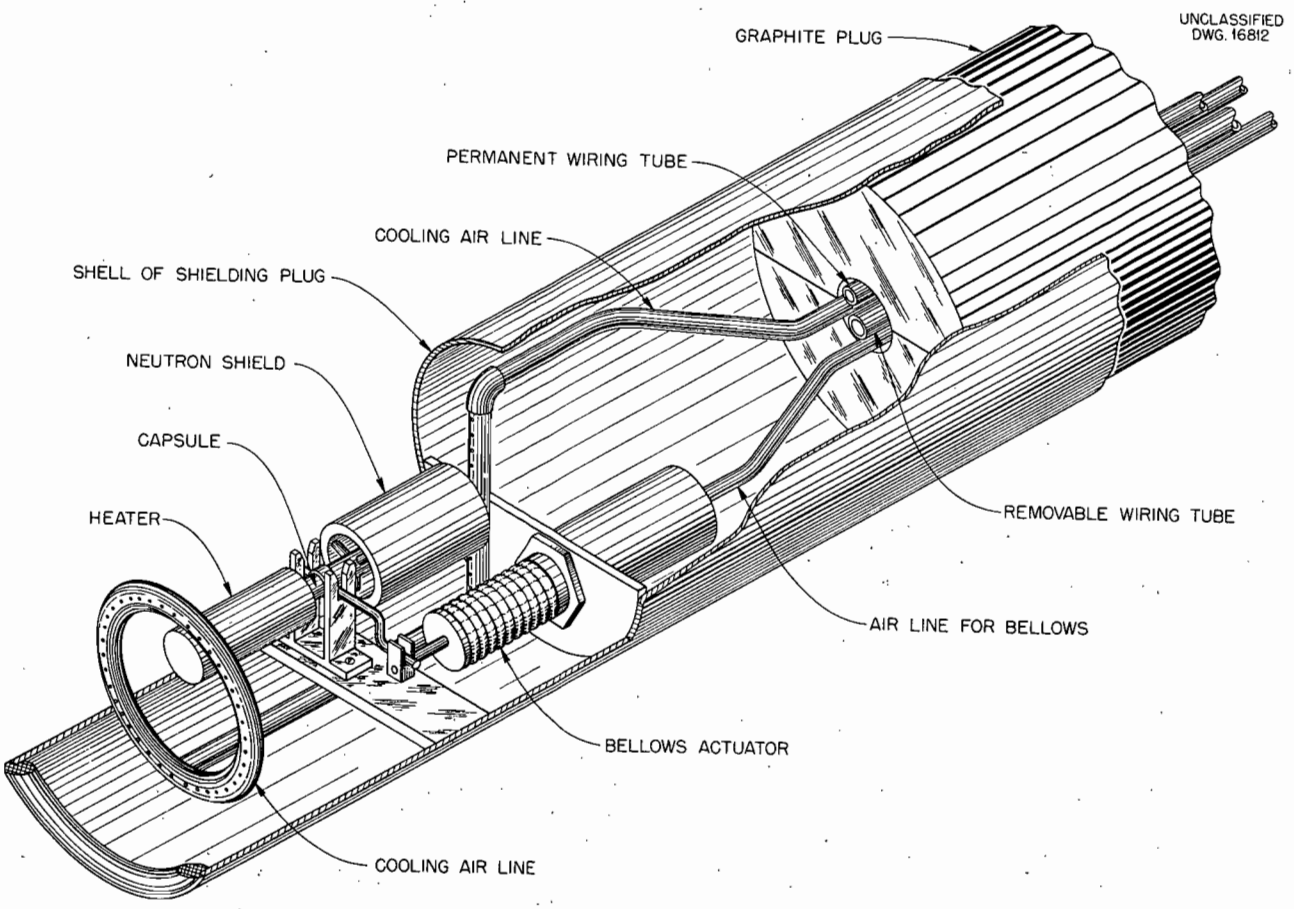

Fig. 20. Dynamic Fuel Testing Assembly.

and the thermal-neutron flux. The thermal-neutron flux at a specified point of observation P may then be expressed in terms of the thermal-neutron flux distribution throughout the medium as

$$\phi_P = \frac{1}{4\pi} \int_{Med.} \frac{\phi}{r^2} \Sigma_s \, e^{-\Sigma_t r} \, dV \quad , \qquad (1)$$

where r is the distance from P to a volume element dV of the medium and the integral extends over all portions of the medium from which thermal neutrons may reach P. In this case, P is the center of the Boral cylinder and the region of integration is limited to the solid angles subtended by the ends of the cylinder at its center. These solid angles include fuel elements of the reactor, as well as a little beryllium and water and part of the plug that closes hole HB-2.

Effective values of Σ_s and Σ_t for a central portion of the fuel element employed in the LITR and the MTR have been computed for use in evaluating the integral of Eq. 1. The necessary information as to the dimensions and composition of the fuel element were either found in the *MTR Handbook* or obtained from J. E. Cunningham of the Metallurgy Division. Cross sections of the constituents for thermal neutrons were taken from *NBS Circular 499*, except in the case of the total cross section of water. For this, the value 86 barns[6] was used. These data lead to

$$\Sigma_s = 1.70 \text{ cm}^{-1} \quad , \qquad \Sigma_t = 1.80 \text{ cm}^{-1} \quad ,$$

indicating that, of the thermal neutrons scattered toward the center of the Boral cylinder from a depth of 2 cm in a fuel element, less than 3% escape. Consequently, the integral of Eq. 1 need not be extended very far into a fuel element.

[6] F. G. Brickwedde, J. R. Dunning, H. J. Hoge, and J. H. Manley, *Phys. Rev.* 54, 266 (1938).

The region of integration will probably not have to be extended very far into the wall of hole HB-2 either and, in the immediate vicinity of the inner end of hole HB-2, the thermal-neutron flux is practically independent of distance measured normally to the axis of the hole.[7] It may therefore reasonably be assumed that the flux varies only with distance z, measured parallel to the axis of hole HB-2; this variation has been measured by J. B. Trice. For use in Eq. 1, however, an empirical expression for $\phi(z)$ is required that conforms with the measurements of Trice. Such an expression, it has been found, is

$$\log \phi(z) = A \cos \frac{z-1}{L-1} \frac{\pi}{2} ,$$

with $A = 13.17$ and $L = 65.9$ inches.

As soon as the geometrical details of the dynamic corrosion test have been finally agreed upon, the evaluation of the integral of Eq. 1 will be undertaken by numerical methods.

[7] Dwg. AED-R-1048, *Thermal Neutron Flux Pattern of the MTR.*

CRYSTAL PHYSICS

ANP REACTOR FUEL-ELEMENT CORROSION UNDER PROTON IRRADIATION

W. J. Sturm R. J. Jones[1]
J. V. Hilyer[1]

Bombardment of liquid eutectic fuels in Inconel has been continued with the resumption of activity of the Y-12 86-in. cyclotron. One of the results of the alterations effected in the several-month shutdown for cyclotron overhaul was an increase in the energy of the proton beam from about 20 to 22.5 Mev.

As had been pointed out in the last report,[2] bombardments of less than 4- to 8-hr duration at 815°C in an energy-dissipation field of as much as 3000 w/cc produced less than 0.0005 in. of corrosion, which is the limit of detection with present methods. A single 8-hr run, however, showed 0.025 in. corrosion of Inconel at the No. 14 eutectic–Inconel interface. Several further 8-hr bombardments have since been carried out with the No. 21 eutectic in Inconel in an effort to obtain data for comparison with the earlier results. The No. 21 eutectic has the following composition: NaF, 4.8 mole %; KF, 50.1 mole %; ZrF, 41.3 mole %; and UF_4, 3.8 mole %.

Of the three 8-hr bombardments thus far completed with eutectic No. 21, chemical analyses and metallurgical examinations have been completed in only one case. Chemical analysis of the bombarded eutectic for trace quantities of the elemental components of Inconel show only a minor increase in the Inconel-component content.

A microscopic metallurgical examination, however, shows significantly increased corrosion in the bombarded portion of the Inconel tubing. This result is shown in Fig. 21*a*. A second Inconel tube was filled with the same batch of eutectic and subjected to the same thermal history in a vacuum furnace, 815°C for 8 hours. A photograph at the same magnification of this eutectic–Inconel interface is shown in Fig. 21*b* and serves as a control for the bombarded specimen. Thus the net effect of the bombardment with 22.5-Mev protons at a power density of about 2500 w/cc has been to increase the depth of corrosion by 0.0015 in., in qualitative substantiation of the results of the last report. It seems safe to conclude that corrosion is enhanced by proton bombardment, although perhaps not at a rate that is excessive for engineering application. More quantitative work is needed to answer this question unequivocally.

[1] Electromagnetic Division, Y-12.

[2] *Solid State Quar. Prog. Rep. May 10, 1952*, ORNL-1301 (in press).

EFFECTS OF THERMAL GRADIENT ACROSS BOMBARDED FUEL ELEMENTS

W. J. Sturm J. V. Hilyer

During the actual proton bombardment, the temperature of the bombarded side of the fuel-element target is controlled and held at 815°C. However, to dissipate the beam energy it is necessary to mount the target on a water-cooled copper tube. As a consequence, the thermal gradient across the target is quite steep, the boundary temperatures being 815 and 10°C. Since the control samples

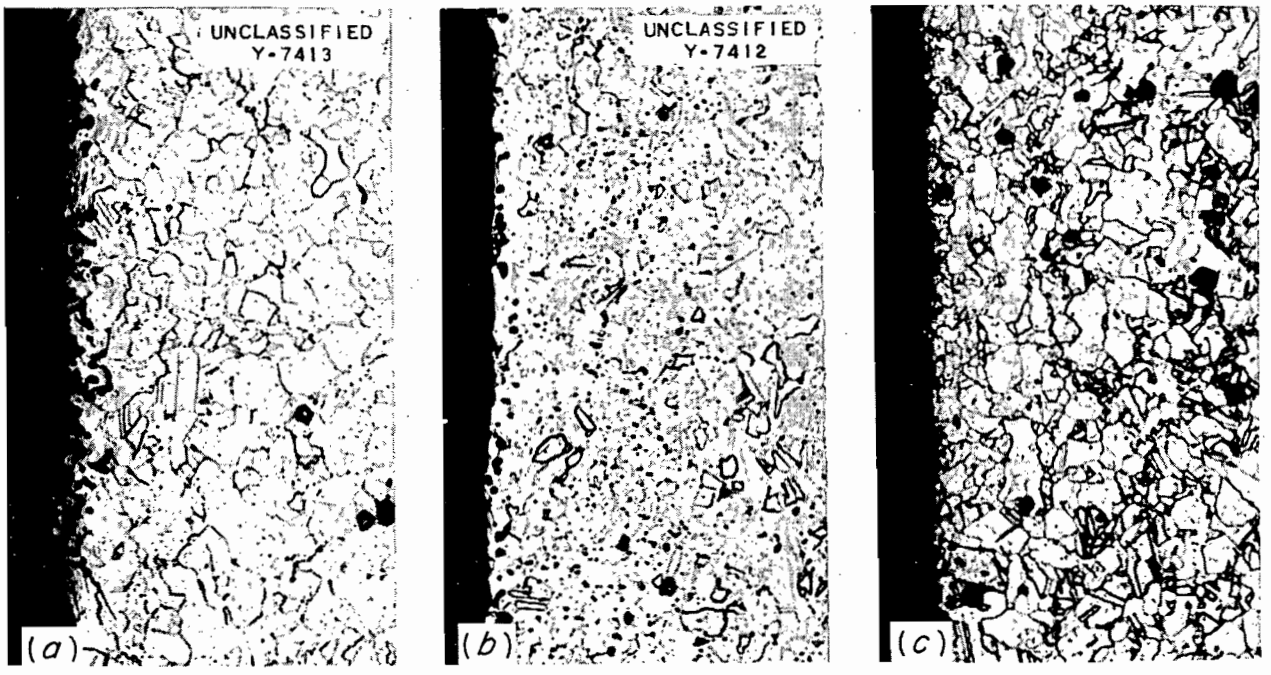

Fig. 21. Corrosion of Inconel by Eutectic No. 21. (*a*) Specimen subjected to 8-hr bombardment at 815°C. (*b*) Specimen held at 815°C for 8 hours. (*c*) Water-cooled specimen.

were uniformly heated in a furnace, they experienced no such gradient. It is therefore possible that the enhanced corrosion observed in the bombarded targets may be a mass transfer of some sort that depends primarily upon this thermal gradient.

To examine this possibility, an Inconel fuel element was prepared and mounted on a water-cooled copper tube. The whole assembly was inserted into the control furnace, the water stream turned on, and the front face of the specimen raised to 815°C. Under these conditions the boundary temperatures were 815 and 40°C. This specimen was held at temperature for 8 hr so that it also served as a control for the bombardment shown in Fig. 21*a*. The water-cooled control sample is shown in Fig. 21c. A variation in the etching and mounting procedures accounts for the difference in appearance of the surfaces, but the region of interest, the surface of the Inconel in contact with the eutectic, is represented equivalently. Although there is no assurance that the nature of the gradient function, aside from boundary conditions, is the same in Fig. 21*a* and c, no evidence of mass-transfer type of corrosion due solely to a thermal gradient is found. The enhanced corrosion rate actually observed in Fig. 21*a* seems to be quite definitely associated with radiation.

It may also be noted that the corrosion induced in the fuel element is found primarily in a region where most of the proton energy dissipation is by ionization. Chemical aspects of corrosion may be expected to be sensitive to ionization, whereas corrosion dependent upon microdiffusion will occur primarily in the region of knocked-on atoms.

INVESTIGATION OF THE CAUSES OF RADIATION CORROSION

W. J. Sturm R. J. Jones

Usually an energetic charged particle such as a proton loses energy in the first part of its range by ionization and excitation of the atoms surrounding its path during its traverse of matter. At lower energy, near the end of its range, the energy exchange is via the knock-on process, in which the atoms of the absorber may be displaced from their lattice sites by the primary particle and by the recoil atoms themselves. Generally, also, the number of secondary particles produced by an energetic light primary particle is very large. Radiation effects are, as determined by measurement of mechanical properties and microdiffusion rates, due to displaced atoms; whereas certain chemical effects, such as dissociation of water and coloration effects, result from ionization. It

is therefore of some interest to try to separate the effects that cause corrosion. If it can be shown that corrosion is enhanced primarily by knock-ons, then the problem of the initiating particle is lessened, since in the last analysis the damage will be caused by the large number of recoil atoms in the target material itself. An experiment designed to separate these effects is being initiated. The energy of transition between excitation-ionization and knock-on is about 10 kev for a proton; that is, above 10 kev the particle loses most of its energy by ionization, whereas below 10 kev most of the energy is lost by knock-on. Hence, a simple absorbing wedge inserted in the proton path ahead of the target, as shown in the lower-right insert of Fig. 22, would result in protons of all energies from 22.5 Mev to zero energy striking the target. A simple metallurgical examination of the target for corrosion as a function of position on the target face should determine whether low-energy protons (knock-ons) or high-energy protons (ionizations) enhance the corrosion rate more.

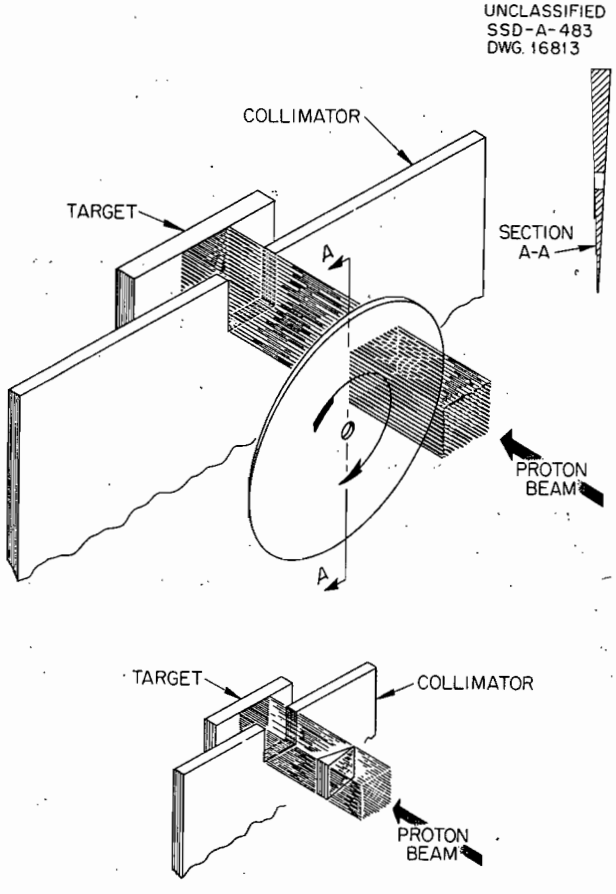

Fig. 22. Apparatus for Study of Corrosion Effects of Protons at Various Energies.

As an alternate approach to the same problem, a preliminary survey has been made of the feasibility of mounting a rotating disk of continuously varying thickness in the proton beam. This system, Fig. 22, would employ a graphite disk of wedge-shaped cross section, the peripheral area of which would attenuate the beam energy. Although this method would produce a distribution of knock-ons throughout the target which is uniform in a first approximation, some difficulty is anticipated in activating an electric motor in the 9000-gauss magnetic field of the cyclotron. Such an energy modulator would prove very useful in many types of radiation-effect studies where the phenomena induced depend upon displaced atoms and in which a uniform distribution of damage in a target is advantageous. Mechanical difficulties may delay the application of the rotating absorber to these problems until the deflection and externalization of the proton beam of the 86-in. cyclotron is accomplished.

HARDENING AND EMBRITTLEMENT OF METALS

D. Binder

Several bombardments of aluminum and copper polycrystalline specimens with 22.5-Mev protons have recently been conducted. The increase in hardness of these samples as a function of depth of proton penetration has been measured. Increases of 20 Tukon numbers were noted in the copper samples; data is not as yet adequate, however, to make a precise plot of this variation possible. In the case of aluminum, a proton bombardment of 100 μamp-hr has not been sufficient to produce more than barely detectable hardening. Longer runs, of the order of 500 μamp-hr, when completed, are expected to show marked hardening in aluminum, and slow-neutron beam transmission measurements will be made to estimate the amount of hydrogen in the sample after bombardment.

METALLOGRAPHIC EQUIPMENT

M. J. Feldman W. J. Sturm

A Vickers projection metallograph equipped for normal and oblique incidence illumination of transparent and opaque objects has been set up in a

temporary location in the Solid State Building. There are two light sources, a carbon arc and a point tungsten lamp, that can be easily interchanged. Polarizer and analyzer filters make the examination of specimens under polarized light possible. Phase contrast and macro equipment will be available ultimately. Photographs have been made with all available illuminations.

Instrumentation for remote mounting, lapping, polishing, etching, examining, and photographing of radioactive specimens is not as yet completed. A separate discussion of these facilities will be made upon their completion several months hence.

THERMAL CONDUCTIVITY OF STRUCTURAL MATERIALS

A. Foner Cohen L. C. Templeton

A radial-heat-flow method was used with an ARE heat-treated specimen of Inconel to make absolute thermal–conductivity measurements as a function of temperature before, during, and immediately following irradiation in hole HB-3 of the LITR. The initial preirradiation measurements were made at six temperatures, the extremes being 130 and 670°C.

The initial part of the in-pile experiment was at about 400°C for 96 hr; the temperature was achieved entirely by gamma heating at a power level of 1500 kw. The temperature of the specimen was then increased to 740°C and maintained at that temperature for a 50-hr interval during which differential temperature measurements were obtained. In this part of the experiment, the differential temperatures used for calculation of the conductivity also include the gamma heating contribution. The reactor power was then reduced to zero for 16 hr and the sample temperature was maintained near 700°C. The reactor power was then raised to a level of 1500 kw and the specimen temperature was increased to 825°C and maintained for a period of about 120 hr. After the irradiation, the reactor power was again reduced to zero, and, when proper experimental conditions were achieved, conductivity measurements were made at four temperatures between 825 and 630°C.

The results of the experiments calculated thus far show that before- and after-irradiation thermal conductivity are the same within the accuracy of the measurements, which is of the order of a few per cent. The data taken during irradiation show no change in the conductivity as a function of time at the constant temperatures mentioned.

Another ARE heat-treated Inconel specimen of similar geometry was subjected to measurements in the LITR for a period of irradiation of the same order as that in the preceding experiment. However, the maximum temperature at which measurements were made was about 700°C. No change in conductivity as a function of irradiation was evident.

Separate experiments will be made in hole HB-3 of the LITR to determine the gamma heating as a function of flux for the various materials of interest. These experiments will also be useful as an independent check on the gamma heating contribution to the differential temperatures measured in the in-pile part of the thermal-conductivity experiments.

A design has been submitted to the shop for construction of equipment to be used in determining the absolute thermal conductivity of metals and alloys, particularly those with conductivity between 0.02 to 0.2 cal/sec·cm·°C. The equipment is for out-of-pile use only. The expected accuracy is hoped to be about 2 or 3% over the temperature range from 100 to 900°C.

CRYOSTAT FOR LOW-TEMPERATURE STUDIES

A. Foner Cohen

A cryostat has been designed for use between temperatures of about 2 and 90°K. With this instrument it will be possible to measure the thermal conductivity of dielectrics, semiconductors, and metals over the entire temperature range provided. In addition, provision for measuring the electrical conductivity of some materials is included. The cryostat will be used primarily in investigating the effect of neutron irradiation on the crystal lattice. For this purpose it is important that the measurement of the thermal conductivity of the crystals of interest be made before and after irradiation. In cases where annealing may occur during the irradiation and afterwards, provisions are made to keep the temperature of the crystal at approximately 80°K during the irradiation and until all the low-temperature measurements are completed. Various details intended to make these features possible have been tested recently. The construction of the cryostat is now in progress.

SPECIAL PROJECTS

MATERIALS IRRADIATION

R. H. Kernohan

Plans were made during the past quarter for the neutron irradiation of a variety of materials prepared by groups outside the Solid State Division.

A series of samples made of two types of oil-hardening tool steels were made by J. H. Erwin under the direction of J. H. Frye of the Metallurgy Division. The samples, consisting of tensile, dynamic modulus of elasticity, and impact samples have been fabricated and labeled. Preliminary testing is nearly complete and the samples will be canned in four slugs to be irradiated at Hanford (Hanford Request No. 166).

R. E. Adams of the Metallurgy Division has made samples of thorium metal to be irradiated in the LITR. These samples are now being bench tested for thermal conductivity, dynamic modulus of elasticity, electrical resistivity, and hardness. Containers have been made that will be suitable for holding the thorium specimens in a helium atmosphere in the high-flux region of the LITR. Preliminary plans were also made for irradiation of thorium metal in the MTR.

Hanford Request No. 167 has been submitted and the containers have been designed and made for the irradiation of 10 disks, each of 32 types of ceramic materials. The samples are being prepared by J. R. Johnson of the ceramics section of the Metallurgy Division.

Three new samples of the graphite-UO_2 specimens made by Battelle and previously reported[1] are being bench tested. These samples will be placed in the ORNL graphite reactor for a very short (6- to 12-hr) exposure.

The irradiation of Fe_2O_3 powder exposed in the LITR for two weeks was studied by E. O. Wollan of the Physics Division for antiferromagnetic effects. No changes were apparent, and there was none of the expected color change in the Fe_2O_3 powder or the quartz capsule containing the powder. There is some speculation that gamma heating may have annealed out any radiation effects. Hence, it was decided to irradiate the powder in hole 51 of the ORNL graphite reactor where water cooling is available. This irradiation has just been completed.

EFFECT OF NEUTRON IRRADIATION ON MISCELLANEOUS MATERIALS

M. C. Wittels J. B. Trice

The materials described in this section were irradiated during the period June 10-24, 1952, in hole C-39 of the LITR for a roughly estimated total exposure of 5×10^{18} nvt.

Sample No. 1, of diamond dust, was irradiated in a position $3\frac{1}{2}$ in. above the center of the fuel assembly, and sample No. 2 was irradiated in a position $\frac{3}{4}$ in. above the center of the fuel assembly. Figure 23 is a comparison of a portion of the Debye-Scherus photographs of the control and No. 1 test samples. These specimens showed the following changes upon x-ray investigation:

Lattice constants

Control sample $a_0 = 3.5605 \pm 0.0004$ *kx* units

Test sample

No. 1 $a_0 = 3.5713 \pm 0.0004$ *kx* units

No. 2 $a_0 = 3.5682 \pm 0.0004$ *kx* units

$\Delta a_1 = +0.0108 \pm 0.0004$ *kx* units

$\Delta a_2 = +0.0077 \pm 0.0004$ *kx* units

$$\frac{\Delta V_1}{V_0} = 0.78 \pm 0.10\%$$

$$\frac{\Delta V_2}{V_0} = 0.65 \pm 0.10\%$$

The large difference in the lattice expansion of these two samples is of interest because it

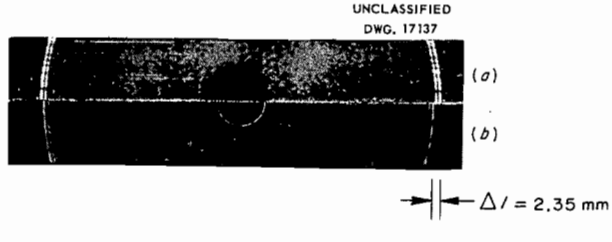

Fig. 23. Back-reflection Debye-Scherrer X-ray Photograph of Diamond Using $Cu_{K\alpha}$ Radiation. Δl = total displacement of (331) line from the zero position.

[1] R. H. Kernohan, *Solid State Quar. Prog. Rep. Jan. 31, 1952*, ORNL-1261, p. 41.

indicates the sensitivity of diamond expansion to fast-flux bombardment. In the initial investigation of this phenomenon, Zachariasen[2] reported $\Delta V/V = 1.00\%$ resulting from an irradiation of several weeks duration at Hanford (190 Mwd/central ton or approximately 6×10^{19} nvt). It therefore appears probable that the expansion is not a linear function of integrated flux. In addition, this expansion probably reaches a maximum at a rather low value. Further tests with diamonds are being conducted to resolve these questions.

[2] W. H. Zachariasen and H. A. Plettinger, *Effect of Neutron Irradiation on Diamond*, ANL-4400, p. 12.

The irradiation of hexagonal silicon carbide under the same conditions as diamond produced no measurable lattice changes. Since the cubic form of silicon carbide was reported[3] to behave similarly to diamond it appears that this relation is structure-dependent.

Preliminary tests indicate that the interstitial compounds ZrN and TiC also undergo lattice expansions, but they are of a lower order of magnitude than that found in diamond. A further investigation of these materials is in progress.

[3] P. Day, L. Fuchs, and W. Primak, *The Density of Irradiated Silicon Carbide*, ANL-4613, p. 31.

Part II

UNCLASSIFIED PROJECTS

CONTENTS

	Page
PART II. UNCLASSIFIED PROJECTS	31
SUMMARY	35
SOLID STATE REACTIONS	36
Low-Temperature Bombardment of Germanium	36
Magnetic Susceptibility of Germanium Semiconductors	39
Hall and Magnetoresistance Effects in Metals	39
Radiation Effects in Ionic Crystals	40
ENGINEERING PROPERTIES	41
Physical Properties of Irradiated Plastics and Elastomers	41
X-ray Studies of Plastics and Elastomers	41
CRYSTAL PHYSICS	46
Effects of Reactor Irradiation on the Properties of Copper Single Crystals	46
X-ray Work	51

SUMMARY

SOLID STATE REACTIONS

Low-Temperature Bombardment of Germanium. Exploratory runs were made in the cryostat recently installed in hole 52 of the ORNL graphite reactor. It was proved conclusively that both *N*- and *P*-type germanium samples retain a considerable amount of lattice damage at temperatures below −100°C but that much of this damage anneals out at room temperature.

Magnetic Susceptibility of Germanium Semiconductors. It was found that the turbulent flow of coolant through the magnet windings of the ADL magnet caused vibrations that prevented accurate force measurements from being made with the supersensitive balance mounted in the magnetic field. Since the present pump was designed to cool a magnet power supply considerably larger than that in actual use, a smaller pump will furnish sufficient cooling for the coils. In addition to using a smaller magnet-cooling pump, an improved mounting system will be used to support the balance. An improvement in microformer circuitry now permits a balance sensitivity of 0.10 μg or better.

Equipment is being built that will maintain low sample temperatures by means of liquid nitrogen. A tentative design has been suggested for extending these temperatures down to the liquid-helium range.

Hall and Magnetoresistance Effects in Metals. Work is nearing completion on measurements of the Hall and the magnetoresistance effects as functions of heat treatment and irradiation in copper-beryllium alloys. Equipment has been assembled for making these measurements, and the area around the magnet has been temperature-controlled to increase the accuracy of the instruments.

Radiation Effects in Ionic Crystals. Measurements made thus far on the effects of radiation on the conductivity of potassium chloride indicate that in-pile irradiation enhances the conductivity in the structure-sensitive region but that some annealing takes place during irradiation. Gamma radiation, on the other hand, decreases the conductivity of potassium chloride crystals. An improved ionic conductivity apparatus is being built for more accurate studies.

ENGINEERING PROPERTIES

Physical Properties of Irradiated Plastics and Elastomers. Plastics and elastomers were found to suffer greater damage per rep from gamma radiation of Au^{198} than from reactor radiation. However, the intensity of the energy absorbed from the reactor was greater by a factor of 100, therefore the greater efficiency attributed to Au^{198} may not hold true if a damage saturation point was exceeded in the case of the reactor. Also, different types of damage were noted for the two kinds of radiation. This was exhibited most effectively in the case of Hycar PA-21, which became softer under irradiation from Au^{198} but became harder under reactor irradiation.

Further data have been obtained on the effects of increased gamma radiation on plastics. The increase in gamma radiation was obtained by reactor irradiation of the samples while enclosed in cadmium. Measurements of gas evolution from irradiated plastics have also been extended to longer irradiation periods.

X-Ray Studies of Plastics and Elastomers. X-ray diffraction patterns were made of a number of plastics before and after various radiation exposures. Some correlation has been found between the change of structure in the plastics and the change in physical properties.

X-ray diffraction studies show that the structures of many nonirradiated polymers can be converted from random to preferred orientation by stretching. This will permit easier detection of changes in future irradiations.

CRYSTAL PHYSICS

Effects of Reactor Irradiation on Properties of Copper Single Crystals. In the study of the theory of radiation effects on metals, copper single crystals were grown in the shape of test specimens. Precise electrical resistivity and density measurements and stress-strain determinations were made on the specimens.

The copper single crystals were irradiated under several conditions of temperature and flux. Since the resistivity measurements show a consistently smaller change for low-temperature determinations than for those made at higher temperatures, an

increase in resistivity produced by reactor irradiation may not be due to an increase in residual resistivity alone. Changes in resistivity are probably the result of displaced atoms. A combination of Seitz's calculations for the number of Frenkel defects to be expected per unit of irradiation and Dexter's estimate of the resistivity that will result from Frenkel defects, produces a value for resistivity that is about twice the observed value. If there is a density change as a result of an exposure of 1×10^{18} nvt, it must be small. The stress-strain curves show a substantial increase in the critical shear stress as a result of reactor bombardment. No appreciable change has been noted after exposure to gamma rays.

X-Ray Work. A G-E power supply has been obtained for the G-E x-ray tube that has been operated from the North American Philips unit in the past. This new installation has been fitted with special attachments for the study of rocking-curve data from copper single crystals.

SOLID STATE REACTIONS

LOW-TEMPERATURE BOMBARDMENT OF GERMANIUM

J. W. Cleland J. H. Crawford
J. C. Pigg

The conductivity of two germanium samples, one *P*-type and the other *N*-type, has been measured during exposure in the cryostat recently installed in the ORNL graphite reactor, hole 52. This was the first experiment to employ the low-temperature facility and was of an exploratory nature; therefore, a low temperature was maintained only periodically during the exposure and during reactor shutdowns in order to investigate various effects of temperature on the electrical properties during varying amounts of bombardment.

The samples were maintained at approximately −145°C immediately before and during the first 16 hr of bombardment to permit the determination of the initial rate of carrier removal and to allow an examination of the initial conductivity behavior. The initial rates of carrier removal for the samples are listed in Table 2 together with the initial characteristics of the two samples. The fast-neutron flux is unknown, therefore the rate of change per incident neutron cannot be determined. At the present time the fast-neutron flux is being estimated by means of the initial conductivity slope of an *N*-type germanium crystal during bombardment at room temperature.

Both samples show a decrease in carrier concentration and it is interesting to note that the rate of removal of electrons from the *N*-type sample is almost exactly twice the rate of removal of holes from the *P*-type sample. If it is assumed that at this temperature the hole traps are completely effective in trapping holes in the *P*-type material (this assumption is not unreasonable), it

TABLE 2. INITIAL RATE OF CHANGE OF CONDUCTIVITY AND CARRIER CONCENTRATION IN GERMANIUM AT −148 ± 1°C

	$\sigma_0^{(a)}$ (ohm^{-1} cm^{-1})	$(d\sigma/dt)_t = 0^{(b)}$ (ohm^{-1}cm^{-1}sec^{-1})	$N_0^{(c)}$ (cm^3)	$(dn/dt)_t = 0^{(d)}$ (cm^{-3}sec^{-1})
N-type	0.905	-4.02×10^{-4}	1.55×10^{15}	-6.35×10^{11}
P-type	2.79	-3.38×10^{-4}	2.16×10^{15}	-3.13×10^{11}

(a) Initial conductivity.
(b) Initial rate of change in conductivity.
(c) Initial carrier concentration.
(d) Initial rate of change in carrier concentration.

can be concluded that, initially, twice as many electron traps as hole traps are introduced per incident neutron. This observation lends added support to the James–Lark-Horovitz[1] model of multiple energy levels associated with both interstitials and vacancies. This model predicts that the net result of the introduction of an interstitial-vacancy pair is the production of two electron traps – (one shallow electron trap near the bottom of the conduction band, estimated to be approximately 0.05 ev deep, and one deep electron trap below the middle of the forbidden band) – and one rather shallow hole trap (if a second hole traps exists, it will be extremely shallow). However, even at this temperature shallow electron traps 0.05 ev deep will be only partially effective in removing holes, and the effect of such a trap will not be great enough to cause a slope difference of exactly two. Thus, if this explanation is valid, the depth of the shallow electron trap as estimated by James and Lark-Horovitz is too small.

The initial linear slope of the bombardment curves for both samples soon gave way to a slight, concave, upward curvature that indicated a tendency toward saturation.

The resistance of the *N*-type sample increased above the limit of measurement of the apparatus ($\sim 10^5$ ohms) after an exposure of about 2 hours. The conductivity of the *P*-type sample decreased by 4 orders of magnitude in 16 hours.

It was obvious that the *N*-type sample had been converted to a *P*-type, since after the samples were warmed to ambient temperature (~30°C) further bombardment caused an increase in conductivity. In addition, the *P*-type sample showed an increase in conductivity, after a total exposure of 24 hr, from an initial value of 0.53 ohm^{-1} to a final value of 1.72 ohm^{-1} at this temperature. Thus the behavior of both samples was according to expectation.

A second low-temperature run was made on the same samples after 36 hours. The temperature maintained was −140 ± 2°C. Both the *N*-type and *P*-type samples exhibited decreases in conductivity. The rate of cooling to the desired temperature was not rapid enough to permit a determination of the initial slopes at the low temperature. However, a decrease in conductivity of the *N*-type germanium was not expected according to the James–Lehman–Lark-Horovitz[2] model. This model would predict an increase in the hole concentration of a sample converted to *P*-type by disorder; the rate of increase would decrease monotonically until saturation was reached. Consequently, it must be assumed that a predominence of hole traps deeper than those observed at the high temperature are introduced at the low temperature. These hot traps are annealed out long before the sample reaches room temperature.

A number of additional low-temperature runs was made during the bombardment period. In these runs care was taken to make sure that the cooling was sufficiently rapid so that the initial slopes of the conductivity vs. bombardment time curves could be measured at the low temperature. The slopes at −140 ± 2°C are listed in Table 3 together with the previous in-pile time.

The most striking feature of the data is that the initial slopes of the *N*-type samples are almost identical and the *P*-type slopes vary less than a

[1] H. M. James and K. Lark-Horovitz, *Z. physik. Chem.* 198, 107 (1951).

[2] K. Lark-Horovitz, *Semiconducting Materials*, p. 74, Academic Press, New York, 1951.

TABLE 3. INITIAL SLOPES AT −140°C AT VARIOUS TIMES DURING EXPOSURE

IN-PILE TIME (hr)	*N*-TYPE SLOPE ($ohm^{-1}cm^{-1}sec^{-1}$)	*P*-TYPE SLOPE ($ohm^{-1}cm^{-1}sec^{-1}$)
84	-1.17×10^{-4}	-2.13×10^{-4}
300	-1.33×10^{-4}	-1.63×10^{-4}
480	-1.19×10^{-4}	-1.69×10^{-4}
495	-1.38×10^{-4}	-1.29×10^{-4}
540	-1.25×10^{-4}	-1.20×10^{-4}

factor of 2 during an exposure period (approximately 22 days), during which the room-temperature conductivity change has strongly approached saturation. The data indicate conclusively that damage is introduced and retained at this temperature and that the damage readily anneals out before ambient temperature is reached. The difference in the *N*- and *P*-type slopes during the early stages of bombardment may be due to a difference in mobility that is subsequently removed as bombardment proceeds, because at the higher exposure period impurity scattering becomes predominant and is expected to be equally effective in both samples. Since the slopes are equal after lengthy exposures, it can be assumed that the effect of the low-temperature annealable damage is the same in both samples.

In order to investigate the kinetics of the annealing process associated with the low-temperature disorder more thoroughly, several runs at a somewhat higher temperature were made. At the higher temperatures (~−100°C) the slight concave upward curvature of the conductivity vs. bombardment plot that was observed at −140°C is accentuated, indicating an increase in the rate of annealing. These curves were fitted with a standard first-order build-up equation of the form

$$\sigma_0 - \sigma = \frac{K}{k'}(1 - e^{-k't}) \quad , \qquad (1)$$

where σ_0 is the initial conductivity at the low temperature and is obtained by extrapolation, K is the initial slope, k' is the first order rate constant, and t is the time. A typical conductivity vs. bombardment curve for the *P*-type sample at −100°C is shown in Fig.24. The points were calculated by using Eq. 1 and $K = 5.92 \times 10^{-3}$ ohm^{-1}cm^{-1}min^{-1} and $k' = 1.43$ min^{-1}. The results of two such runs

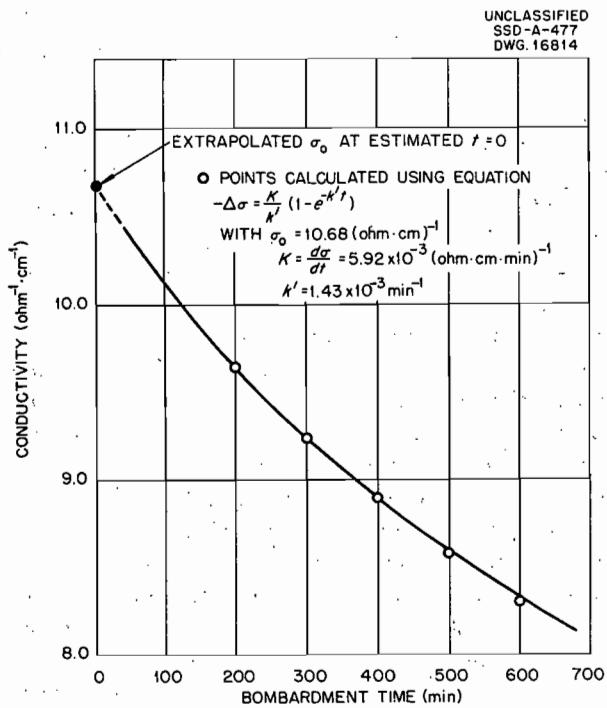

Fig. 24. Conductivity vs. Bombardment at −100 ±2°C for *P*-Type Germanium.

are listed in Table 4. In view of the successful fit of the data, it may be assumed that the annealing process is essentially first order.

The most important conclusion to be drawn from the first exposure of germanium in the cryostat is that there is retention of a considerable amount of lattice damage at low temperatures (below −100°C) and the damage anneals out readily below room temperature. An extensive investigation of this low-temperature damage is planned, particularly with respect to the annealing kinetics. The order of the process will be investigated more thoroughly

TABLE 4. FIRST-ORDER RATE CONSTANTS DETERMINED FROM CONDUCTIVITY VS. BOMBARDMENT

TEMPERATURE (°C)	*N*-TYPE		*P*-TYPE	
	K (ohm^{-1}cm^{-1}min^{-1})	k' (min^{-1})	K (ohm^{-1}cm^{-1}min^{-1})	k' (min^{-1})
−114 ± 2	7.60×10^{-3}	1.07×10^{-3}	8.59×10^{-3}	1.20×10^{-3}
−100 ± 2	5.79×10^{-3}	1.50×10^{-3}	5.92×10^{-3}	1.43×10^{-3}

and attempts will be made to determine the activation energy or distribution of activation energies for the process. It may be possible, from the latter information, to draw inferences concerning the mechanism of the process and the nature of fast-neutron produced disorder introduced under conditions that permit a minimum of atomic rearrangement immediately after the collision.

MAGNETIC SUSCEPTIBILITY OF GERMANIUM SEMICONDUCTORS

D. K. Stevens

A study of the vibration problem associated with the ADL magnet indicated that the major source of the vibrations was the turbulent flow of liquid coolant through the magnet windings. The present cooling system is designed to dissipate heat generated when the magnet is supplied by 125 kw of electrical energy, but the converter now in use is rated at only 25 kw. Therefore the present pump may be replaced satisfactorily by one producing a much lower flow rate. This pump is now on order.

In order to further reduce the vibration problem, a system of mounts for the balance has been devised that greatly reduces mechanical oscillations reaching the balance. The mounting consists of a system of critically loaded rubber mounts and an intermediate mass. The high flow rate of the coolant can almost be tolerated with this mount. Thus, the substitution of a smaller coolant pump is expected to permit the mounting of the balance and its associated vacuum system directly on the magnet. Braces are now being made for this purpose.

An iron bell-jar system and a liquid-nitrogen cryostat have been designed and construction is approximately 90% complete. The cryostat consists of a $^3/_4$-in., closed-end, copper sample tube surrounded by a metal vacuum jacket that also contains a reservoir of liquid nitrogen. This copper tube is joined to the bell-jar system by means of a 0.010-in.-wall copper-nickel tube that also provides thermal isolation. A copper foil connects the sample tube to the refrigerant vessel. Temperatures above that of the refrigerant will be obtained by means of a short electric heater winding located below the copper foil on the copper tube. Thus, the temperature of the isolated copper tube below the heater is determined by the temperature of these windings. An atmosphere of helium at a pressure of approximately 0.2 mm Hg will provide heat transfer between the suspended sample and the walls of the tube.

As previously described,[3] the position of the balance beam is indicated by means of a linear differential transformer (microformer). The output of this instrument is amplified and fed into a phase-sensitive detector that compares the phase of the output signal with that of the exciting frequency. As the core moves through the linear differential transformer, the amplitude of the output signal should reduce to zero and then increase again with a phase shift of 180 degrees. It was found necessary to place a condenser across one of the output coils to achieve this type of operation, a measure that also resulted in an approximately tenfold increase in detection sensitivity. At present the balance appears to have a sensitivity of $^1/_{10}$ μg or better.

The necessity of placing a condenser across one of the secondary coils clearly implies that the microformer lacks symmetry. Further evidence of this fact is the high sensitivity of the system as a whole to the frequency and amplitude of the driving signal of the microformer. It has been shown that when the core is located so as to produce a minimum output signal, a force that varies with the frequency and amplitude of the excitation signal is exerted on the core. It was found that this effect could be greatly diminished by placing a piece of iron in a fixed position near one of the secondary coils. Presumably, the equilibrium position of the core relative to primary was made to coincide with that of the secondaries.

Serious thought is being given to building suitable equipment for the extension of measurements to temperatures in the liquid-helium range. A tentative design for such equipment has been suggested by J. G. Daunt of Ohio State University.

HALL AND MAGNETORESISTANCE EFFECTS IN METALS

A. B. Lewis

An investigation of the Hall and the magnetoresistance effects in metals, particularly the beryllium-copper type alloys, as a function of heat treatment and irradiation damage has been

[3] *Solid State Quar. Prog. Rep. May 10, 1952*, ORNL-1301 (in press).

proposed. The Hall effect will be measured with a potentiometer in the conventional manner. The magnetoresistance effect will be measured by comparison of the resistance of a specimen in the magnetic field with that of an identical specimen outside the magnetic field, by means of a Kelvin bridge.

A conventional Kelvin bridge has been assembled from components available in the laboratory. This bridge appears to be reliable to one part in ten thousand and has a sensitivity of two or three parts in the next decimal place. Up to now, air drafts and temperature fluctuations appear to have set the limits of reproducibility of the bridges. To eliminate this difficulty, the area around the magnet is being enclosed and temperature-controlled. The work is nearing completion.

RADIATION EFFECTS IN IONIC CRYSTALS

R. L. Sproull R. S. Caswell

Measurements of the effect of neutron and gamma radiation on the conductivity of potassium chloride are in progress. The ionic-conductivity apparatus described in the previous report[3] is being employed; in addition, an improved ionic-conductivity apparatus is under construction in the shop. There are three chief improvements in the new apparatus. The apparatus may be evacuated, eliminating the "background" current due to ionization produced in the helium atmosphere of the present apparatus by the radioactivity of the crystal, the new apparatus may be placed in a hot-oil bath for constant-temperature annealing runs at relatively high temperatures, and a vibrating-reed electrometer will be used for increased current sensitivity.

A number of qualitative conclusions may be drawn from the crystals studied thus far.

1. Irradiation in the pile enhances the conductivity of the crystal in the structure-sensitive (low temperature, for example, below 200°C) region.

2. Enhancement of the conductivity is not proportional to the integrated neutron flux at about 10^{18} $(nvt)_{fast}$, but is less, indicating that some annealing is taking place during irradiation in the pile.

3. Co^{60} gamma radiation decreases the conductivity of the potassium chloride crystals.

4. The order of the annealing process, by which the enhanced conductivity is removed, cannot be determined from present data without ambiguity. It is hoped that a study of the annealing process over a wide range of temperatures with the new apparatus will clear up this situation.

ENGINEERING PROPERTIES

PHYSICAL PROPERTIES OF IRRADIATED PLASTICS AND ELASTOMERS

C. D. Bopp R. L. Towns
O. Sisman W. K. Kirkland

Further results on the relation between the damaging effects of gamma radiation from Au^{198} and reactor radiation[1] are given in Table 5. The dosage values in rep, calculated by the method previously described,[2] include the energy absorbed from fast neutrons as well as the energy absorbed from gamma radiation.

The energy absorbed during exposure to gamma radiation from Au^{198} is more efficient in producing changes than the energy absorbed during exposure to reactor radiation. Such a trend was observed in the earlier results only for the less resistant materials, however, the previous exposure was not sufficient to cause extensive changes in the more resistant materials. Extensive changes are shown by all the materials reported here for the longer exposure period.

Since the intensity of the energy absorbed (rep/hr) was a hundred times greater for the reactor radiation than for the Au^{198}, it is speculated that the greater efficiency for the Au^{198} in producing damage is due to the lower dose rate. This assumption is based on the premise that more recombination of ions occurs at the higher radiation intensities and less damage results. It appears that in some instances the nature of the damage is somewhat different for the two kinds of radiation. An example of this can be seen in Table 5 where Hycar PA-21 becomes softer under radiation by Au^{198}, whereas, for an equivalent decrease in tensile strength by reactor radiation, the material has become harder than when unirradiated. Further investigations of this effect will be made.

Test results given in Table 6 indicate that some of the more resistant plastics are only slightly damaged at 3×10^{10} rep (from 3 to 8 times greater than previous exposures). The time of exposure was the same as before (about six months), but the plastics were wrapped in cadmium sheet. The flux of gamma radiation is increased by a factor of about 9[1] by the (n,γ) reaction with thermal neutrons; however, the fast-neutron flux is not changed significantly. For polyethylene, which absorbs 2.5 times more energy from fast neutrons than from gamma radiation, the increase in the total energy absorbed is about threefold when wrapped in cadmium. For plastics containing less hydrogen than does polyethylene, a larger fraction of the total energy is from gamma radiation and the increase is greater.

The volume of gas evolved by irradiated plastics for reactor exposures longer than reported previously is listed in Table 7.

X-RAY STUDIES OF PLASTICS AND ELASTOMERS

C. D. Bopp G. E. Klein
F. A. Sherrill

Certain radiation-produced changes in plastics and elastomers can be related to the chemical structure. X-ray diffraction patterns are being studied to help establish the nature of these changes. A description of the x-ray diffraction patterns for a few plastics is given in Table 8.

The following types of soft materials will harden under radiation:

1. materials with the $(CH_2)_n$ structure of polyethylene,
2. similar materials in which part of the carbon is replaced by nitrogen,
3. materials in which one of the hydrogen atoms attached to some of the carbon atoms is replaced by an organic radical.

However, the following soft materials are found to become still softer under irradiation:

1. materials in which the polyethylene type of structure is changed in that oxygen or sulfur replace part of the carbon,
2. materials in which both of the hydrogen atoms attached to some of the carbon atoms are replaced by organic radicals,
3. materials in which part of the hydrogen is replaced by halogen.

The gas evolved during irradiation is less for plastics with structures in which aromatic groups replace part of the hydrogen of the $(CH_2)_n$ chain. It is supposed that less fragmentation of the molecules occurs for the aromatic-substituted

[1] C. D. Bopp, O. Sisman, R. L. Towns, and W. K. Kirkland, *Solid State Quar. Prog. Rep. Oct. 31, 1951*, ORNL-1214, p. 39.

[2] O. Sisman and C. D. Bopp, *Physical Properties of Irradiated Plastics*, ORNL-928 (June 29, 1951).

TABLE 5. COMPARISON OF CHANGES PRODUCED BY THE GAMMA RADIATION FROM GOLD-198 AND RADIATION FROM THE ORNL GRAPHITE REACTOR

Conditions: a. Not irradiated
b. Au^{198} irradiated (1.5×10^4 rep/hr)
c. Reactor radiation equivalent to Au^{198} irradiation (10^6 to 3.5×10^6 rep/hr)

TYPE OF TREATMENT	MATERIALS IRRADIATED				
	Butyl Rubber	Hycar PA-21	Thiokol ST	Nylon FM-10001	Royalite (butadiene-styrene copolymer)
Dosage (rep)					
a		0	0	0	0
b	8×10^7	8×10^7	8×10^7	8×10^7	8×10^7
c	$> 10^8$	3×10^8	2×10^8	2×10^8	2×10^8
Tensile strength (lb/in.^{2})					
a		1900	800		
b	Tarry mass	200	350		
c	Tarry mass	800	480		
Shear strength (lb/in.^{2})					
a				11,000	5500
b				9,000	8200
c				9,000	7400
Elongation (%)					
a		300	150		
b		60	100		
c		20	60		
Durometer hardness					
a		65	75		
b		52	69		
c		78	73		
Rockwell hardness					
a scale					
a				66	71
b				78	84
c				80	84
R scale					
a				98	92
b				104	102
c				105	92

TABLE 6. CHANGES PRODUCED BY PILE IRRADIATION FOR 1.3×10^{19} nvt IN CADMIUM (about 3×10^{10} rep)

Conditions: a. Not irradiated
b. Irradiated for 1.3×10^{19} nvt

TYPE OF TREATMENT	MATERIALS IRRADIATED*				
	Polystyrene	Polyvinyl carbozole	Aniline formaldehyde	Karbate (phenolic bonded graphite)	Fabric-asbestos phenolic
Tensile strength (lb/in.^{2})					
a	6000	2000			
b	6000	2000			
Impact strength (lb/in. notch)					
a			0.27	0.27	3.9
b			0.27	0.27	3.6
Elongation (%)					
a	1.4	0.3			
b	1.4	0.3			
Elastic modulus					
a	4.8×10^5	6×10^5			
b	4.8×10^5	6×10^5			
Specific gravity (25/25°C)					
a	1.046	1.19	1.205	1.70	1.70
b	1.076	1.19	1.205	1.70	1.64
Change in weight (%)					
a	0				
b	1.7				
Increase in weight (%)					
a			0	0	0
b			0.50	0.25	–3.3
Rockwell hardness					
a scale					
a	105	113	107	90-110	121
b	96-102	113	106	90-110	106
R scale					
a	122	125	128	90-110	120
b	116-120	125	124	90-110	112

*Formulas and compositions listed in reference 2.

TABLE 7. VOLUME OF GAS EVOLVED FROM IRRADIATED PLASTICS

MATERIAL*	EXPOSURE					
	4.7×10^{18} nvt		1.2×10^{19} nvt		1.0×10^{19} nvt (with cadmium)	
	Dosage (rep)	Gas (ml/g)	Dosage (rep)	Gas (ml/g)	Dosage (rep)	Gas (ml/g)
Polyethylene	5×10^9	116	1×10^{10}	235		
Polyvinyl formal	3×10^9	86	8×10^9	135		
Plaskon alkyd (mineral filler)	**	3	**	19	**	29
Royalite (butadiene-styrene copolymer)	**	3	**	6		
Aniline formaldehyde	3×10^9	1	8×10^9	6	3×10^{10}	11
Amphenol (polystyrene)	3×10^9	0	8×10^9	0	3×10^{10}	5
Styron 475 (polystyrene)	3×10^9	0	8×10^9	0		
Duralon (furfural alcohol polymer with mineral filler)	**	0	**	0		
Fiber-asbestos phenolic	**	0	**	0		
Haveg 41 (phenolic-bonded asbestos)	**	0	**	0		
Karbate (phenolic-bonded graphite)	1×10^9	0	3×10^9	0	3×10^{10}	0

*Formulas and compositions of materials are listed in reference 2.

**The exact amount of mineral filler was not known for these materials so the rep dosage was not calculated.

materials. Since no lessening in the rate of radiation-hardening of soft materials is effected by aromatic substitution, it is speculated that the hardening process is not related to fragmentation.

Changes observed in the x-ray diffraction patterns are listed in Table 8. The materials listed in Table 8 are grouped in the manner in which mechanical properties change upon irradiation as follows:

Group A. soft plastics that harden upon irradiation at exposures $< 10^9$r,

Group B. plastics that soften at exposures $< 10^9$r,

Group C. hard plastics that crumble at exposures $< 10^8$r,

Group D. hard plastics that do not change markedly for exposures $< 10^{10}$r.

The plastics studied in group A showed pattern changes. Further study is planned to see if the pattern changes may be related to changes in structure. Plastics in group B showed no change except for exposures sufficiently long to produce chemical decomposition, as evidenced by fluids seeping out of the materials. Plastics in group C showed no change until weakened mechanically to the point of crumbling. Plastics in group D show less change than group A plastics although change is shown for very long exposures when the mechanical properties are affected.

TABLE 8. EXAMINATION OF IRRADIATED PLASTICS BY X-RAY DIFFRACTION

GROUP	MATERIAL	APPEARANCE OF PATTERN BEFORE IRRADIATION	IRRADIATION EXPOSURE (equivalent roentgens)	CHANGE IN PATTERN AFTER IRRADIATION
A	Polyethylene	2 sharp peaks, several minor peaks	2.2×10^9	Coalition of 2 sharp peaks, diminution of intensities of minor peaks
A	Nylon FM-10001	Double peak, halo	1.7×10^9	Change in nature of double peak, shift in halo position
B	Polyvinyl formal	1 broad band	1.6×10^9	No change
B	Polyvinyl formal	1 broad band	25×10^9	Increase in half-width, diminution in intensity
B	Vinyl chloride acetate	Broad halo	1.0×10^9	No change
C	Teflon	Crystalline	0.06×10^9	No change
C	Teflon	Crystalline	0.58×10^9	Slight increase in peak sharpness, shift in parameters
C	Fluorothene	1 broad peak, 1 halo	0.06×10^9	No change
D	Aniline formaldehyde	1 broad peak	27×10^9	Increase in half-width of peak, diminution in intensity
D	Polyvinyl carbazole	1 broad peak, 1 sharp line	25×10^9	No change
D	Polystyrene	Diffuse peaks	29×10^9	Slight increase in lattice dimensions, general broadening of peaks

X-ray diffraction studies on unirradiated materials show, for many polymers that have been stretched, a partially crystalline structure, but often the unstretched polymers give semiamorphous patterns. It appears that randomly arranged crystallites become oriented upon stretching. For this reason it is planned also to study materials in which the molecules have been oriented by stretching or by casting in thin films to produce more crystalline material from which x-ray information can be obtained with greater ease.

Some patterns for elastomers were also examined, but the pattern produced by the crystalline fillers interfered with the halo patterns of the polymer. It is planned to obtain the patterns for the filler material separately in order to separate the changes in the filler from changes in the polymer patterns.

CRYSTAL PHYSICS

EFFECTS OF REACTOR IRRADIATION ON THE PROPERTIES OF COPPER SINGLE CRYSTALS

T. H. Blewitt R. E. Jamison
R. R. Coltman J. K. Redmond

Before the development of the first reactor, E. P. Wigner suggested that fast neutrons would change the properties of solids. This would result from the fast neutrons knocking on the atoms and displacing them from the lattice sites. Theoretical studies of the phenomenon can be made from two different viewpoints: the history of each incident neutron may be followed as has been done by F. Seitz,[1] or it may be assumed that the energy of the displacement atom is dissipated in heat and the observed changes in properties arise from a localized high-temperature region often called a thermal spike. H. Brooks has made a theoretical study[2] using the latter viewpoint.

In the case of metals, the atom displaced by the neutron, the primary knock-on, will in general dissipate its energy by either excitation or ionization of the conduction electrons or by an elastic type of collision with the atoms of the metal. Seitz, by using the Fermi-Thomas atom and the Born approximation to estimate the scattering cross section for each of these processes, found that the ratio of the rate of dissipation of energy of of these two processes is given by

$$\frac{\left(\frac{dE}{dx}\right)_{\text{collision}}}{\left(\frac{dE}{dx}\right)_{\text{excitation}}} = \frac{Z^{10/3}}{3n} - \frac{m}{M}\,\frac{E_{r_2}^2}{E}\,\frac{\log\frac{E_0}{E^*}}{76.2}\ , \qquad (1)$$

where Z, n, m, M are the usual notations for the atomic number, number of free electrons, mass of the electron, and mass of nucleus, E_r is the Rydberg energy, $2E$ is the product of the mass of the electron and the square of the velocity of the displaced atom, E_0 is the energy of the displaced atom, and E^* is given by $32\ Z^{2/3}\ (m/M)$ ev.

In the case of copper, this ratio has a value of the order of 30 when E_0 is taken as the average energy of a primary knock-on from a 2-Mev neutron. On the basis of the approximation used by Seitz, the energy of a displaced atom produced by a fission neutron in copper will be dissipated mainly by elastic collisions.

The number of displaced atoms per primary knock-on for copper may be estimated from Seitz's approximation. Assuming one tertiary knock-on per secondary knock-on, the number of displaced atoms per primary displacement will be given by

$$N_d = \frac{E_0}{E_d \log E_0}\ , \qquad (2)$$

where E_d is the energy to displace an atom from its lattice site (25 ev). For the average value of a primary knocked-on copper ion by a 2-Mev neutron, Eq. 2 gives a value of 380. Since the number of primary knock-ons will be given by

$$N_p = N_0\ (\text{nvt}) \times \sigma_s\ , \qquad (3)$$

where N_0 is the number of copper ions, nvt is the number of neutrons per cm^2, and σ_s is the scattering cross section. σ_s can be assumed to be approximately 3 barns, so that the fraction of primary knock-ons will be given by

$$\frac{N_p}{N_0} = 3 \times 10^{-24}\ (\text{nvt})\ .$$

It should be noted that, since the number of primary knock-ons is the same order as the number of neutrons, it is permissible to take E_0 in Eq. 2 as the energy arising from knock-on by a 2-Mev neutron. The total number of displaced atoms in copper will then be given by

$$N_D = N_d \cdot N_p = 380\ (\text{nvt}) \times 3 \times 10^{-24}\ N_0\ ,$$

or

$$\frac{N_D}{N_0} = 1.1 \times 10^{-21}\ (\text{nvt})\ .$$

In order to examine this theory of Seitz, measurements of the electrical resistivity and density were made, and the results will be interpreted in the light of the developments of Seitz that are indicated above. Stress-strain curves were also determined for the same samples used for the determination of the electrical resistivity and the

[1] F. Seitz, *Trans. Faraday Soc.* 5, 271 (1949).

[2] H. Brooks, *The Thermal Spike Picture of Radiation Damage*, KAPL-360 (Aug. 4, 1950).

density. More detailed work on the mechanical properties will be reported in a succeeding paper.

Single crystals were grown in the shape of tensile-test bars by the Bridgeman technique, under a vacuum of 10^{-4} mm or less, from spectrographically pure copper (99.999%) furnished by American Smelting and Refining Company. The graphite crucibles that were used were carefully split to remove the samples. The nominal dimensions of the samples are indicated in Fig. 25.

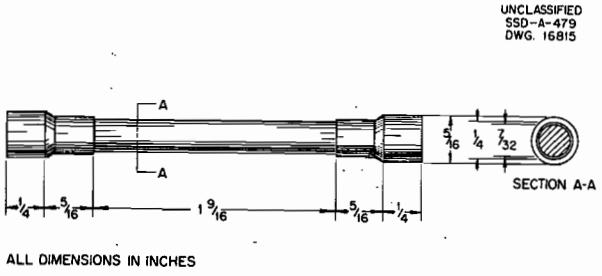

Fig. 25. Copper Single-Crystal Test Specimen.

The cross-sectional area was chosen so as to be convenient for the measurement of the density, electrical resistivity, and the mechanical properties by the use of available equipment.

After the crystals were grown they were etched with 1:1 HNO_3, and their orientation was determined by the Laue back-reflection technique. They were then annealed in a vacuum of 10^{-5} mm at 950°C for 1 hour.

The electrical resistivity of the sample was measured by allowing a known current to flow through the specimen and then measuring the potential drop between two probes. A schematic diagram of the apparatus is shown in Fig. 26. Five readings were made with the current flowing in each direction to eliminate the effect of spurious emf's. The readings were made alternately and the temperature was determined by a copper-constantan thermocouple immediately before and after each set of readings.

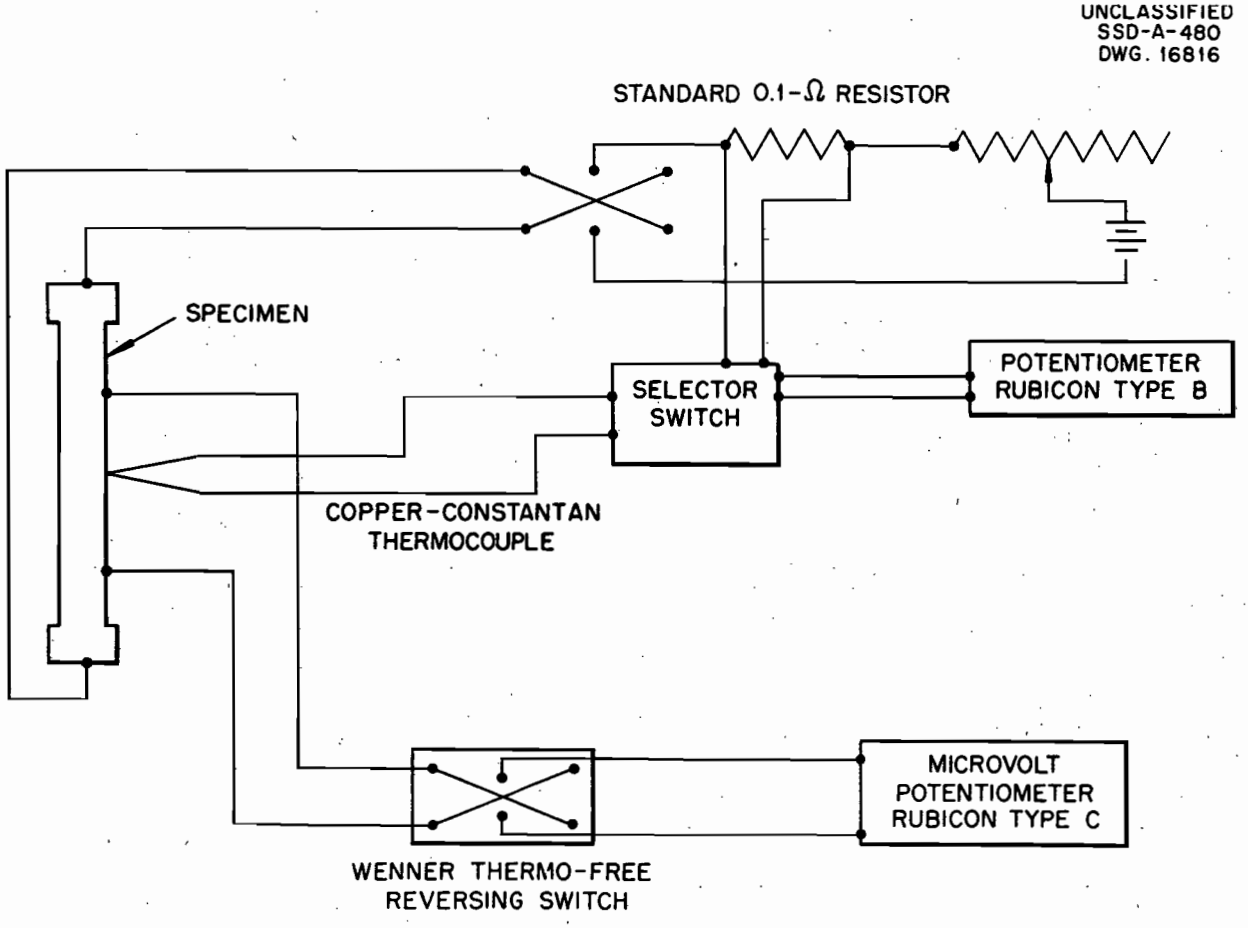

Fig. 26. Schematic Diagram of Electrical Resistivity Apparatus.

The resistance was determined at two temperatures. Samples were immersed in a bath of acetone to obtain a measurement in the vicinity of 20°C. They were also immersed in a bath of boiling nitrogen to obtain determinations at −196°C. For the measurements at 20°C two sets of readings were made with a current of 1 and 2 amp, respectively, while at −196°C the two sets of readings were made at 4 and 5 amperes.

The probes used to determine the electrical potential in the earlier measurements, samples 3*A*, 3*B*, *T*1, and *T*2, were razor blades held in position by nylon clamps. The razor blades left small scratches on the specimens and the distance between the scratches was then determined with a toolmaker's microscope. Later measurements on samples 17*A*, 19*A*, 14*B*, 16*A* and 21*A* were made with leads that were 40-gage copper wires sintered to the sample by the simple process of allowing the weight of the sample to rest on the wire during the high-temperature anneal. At least two determinations were made on each type of sample, and the specimen was removed from the apparatus between measurements to check reproducibility.

The density was determined by hydrostatic weighing in carbon tetrachloride. In order to eliminate the measurement of temperature, the density of the samples was compared to the density of a gold bar. It was assumed that neither the mass nor the density of the gold bar changed with time. The weights of the samples and the gold bar were determined alternately in the liquid. Since these weighings were made rapidly, it was only necessary to assume that the density of the liquid remained constant for a short time.

Samples 3*B*, *T*1, and *T*2 were sealed in evacuated quartz tubes, placed in an aluminum tube, and bombarded in the ORNL graphite reactor. The experimental facility in this reactor was equipped with an enriched-uranium doughnut that converts thermal neutrons to neutrons with fission energy. The ambient temperature was maintained at 25°C by water cooling. The fast flux in the facility is about 5×10^{11} neutrons/cm^2·sec.

The bombardment of samples 17*A*, 19*A*, 14*B*, 16*A* and ~~19*B*~~ was made in another facility in the reactor. The facility had a natural uranium converter and was AIR ~~water~~-cooled to an ambient temperature of 40°C. The fast flux in this facility is about 1×10^{12} neutrons/cm^2·sec. The duration of the bombardment was 28 days. The samples were not sealed in a vacuum.

Samples 19*A* and 21*A* were bombarded in a cobalt gamma source for two weeks. The exposure was equivalent to 3.28×10^9 r, which is estimated to be the exposure received in the graphite reactor for a one-month irradiation. The samples were exposed to air during bombardment.

After irradiation, the resistivity data for samples 3*A*, 3*B*, *T*1 and *T*2 were treated in a somewhat different manner from those of samples 17*A* and 19*A*, 14*B*, 16*A*, 21*A* because of the different manner in which the potential probes were fixed. In the former case, the potential probes were removed after each determination, and the difficulties associated with the accurate measurement of the effective length and diameter of the samples prevented the determination of the resistivity to the desired accuracy. As a result, it was assumed that the temperature-dependent part of the resistivity was unaffected by the reactor bombardment and the ratio of area to length was determined by adjusting the mean temperature coefficient, between 20°C and −196°C, to a constant. The final results for these samples are thus reported with a resistivity in reference to one determination of sample 3*B* and a mean temperature coefficient adjusted to equal that of the first determination of sample 3*B*.

The resistivity data of samples 17*A* and 19*B* are treated in a straightforward way. The differences in resistivities of these samples probably arise from errors made in measuring the cross-sectional area.

Examination of the data in Table 9 shows that the electrical resistivity increased about 0.2% for a bombardment of 1×10^{18} nvt, whereas Table 10 shows a similar increase for a bombardment of 2×10^{18} nvt. The data of Table 10 are probably more reliable. The latter data also offer evidence that the increase in resistivity may not be due to an increase in residual resistivity alone, because the results show a consistently smaller change in resistivity for the low-temperature determinations than for the high-temperature readings. Table 10 also shows that gamma rays, as one may suspect, will not change the electrical resistivity of copper.

It is pertinent to consider whether all the resistivity change observed is attributable to displaced atoms and is associated with observed changes in mechanical properties. The effect of transmutations should first be considered. If neutron capture occurs, the copper atoms can be converted to either zinc or nickel. The number of transmutations can be estimated from the capture

TABLE 9. CHANGE IN RESISTIVITY OF COPPER SINGLE CRYSTAL AFTER IRRADIATION

ρ_{RT} = resistivity at room temperature in microhm-centimeters
ρ_{LN} = resistivity at liquid-nitrogen temperature in microhm-centimeters
ΔT = difference in temperature between ρ_{RT} and ρ_{LN}
$M \times 10^{-3}$ = average temperature coefficient of resistivity between 90 and 300°A
ρ'_{RT} = resistivity at room temperature, adjusted for error in geometry, in microhm-centimeters
ρ'_{LN} = resistivity at liquid-nitrogen temperature, adjusted for error in geometry, in microhm-centimeters
ρ'_{20} = resistivity reduced to 20°C in microhm-centimeters
$\Delta\rho'_{20}$ = difference in resistivity at 20°C from that of the first measurement of sample 3B
$\Delta\rho'_{20}$ (avg) = average change in resistivity

SAMPLE	ρ_{RT}	ρ_{LN}	ΔT	$M \times 10^{-3}$	ρ'_{RT}	ρ'_{LN}	ρ'_{20}	$\Delta\rho'_{20}$	$\Delta\rho'_{20}$ (avg)
Before Irradiation									
3B	1.6621	0.19208	221.22	6.6497			1.6639		
3B	1.6802	0.19358	223.825	6.6419	1.6822	0.19381	1.6658	0.0019	
T2	1.68375	0.19593	221.08	6.7298	1.6637	0.19360	1.6671	0.0032	
T2	1.70825	0.19720	224.06	6.7440	1.6844	0.19444	1.6663	0.0024	
T1	1.59080	0.18407	221.92	6.3389*	1.6688	0.19309	1.6664	0.0025	
T1	1.70585	0.196045	223.69	6.7495	1.6806	0.19314	1.6651	0.0012	
3A	1.6929	0.19884	223.03	6.6989	1.6805	0.19738	1.6772	0.0133	
3A	1.7042	0.19894	223.77	6.7268	1.6847	0.19666	1.6689	0.0050	
After Irradiation with 2×10^{18} nvt; sample 3A Unirradiated									
3B	1.65215	0.19810	218.94	6.6413	1.6542	0.19835	1.6696	0.0057	
3B	1.6497	0.19800	218.37	6.6479	1.6501	0.19805	1.6686	0.0047	+0.0042
T2	1.6768	0.19954	219.44	6.7321	1.6563	0.19710	1.6689	0.0050	
T2	1.6734	0.19999	219.17	6.7226	1.6553	0.19782	1.6692	0.0053	+0.00235
T1	1.6754	0.20029	219.01	6.7353	1.6541	0.19774	1.6701	0.0062	
T1	1.6907	0.20051	221.25	6.7354	1.6692	0.19796	1.6700	0.0061	+0.0048
3A	1.6695	0.19708	220.18	6.6873	1.6601	0.19597	1.6688	0.0049	−0.0008
3A	1.6757	0.19835	219.43	6.7324	1.6551	0.19591	1.6674	0.0035	

*Knife edge mark doubtful.

cross section. A liberal estimate for the capture cross section for energies greater than thermal energies is 3 barns. From this value, the fraction of atoms that are transmuted is given by

$$\frac{N_t}{N_0} = \sigma_c \times \text{nvt} = 3 \times 10^{-24} \times 2 \times 10^{-18}$$
$$= 6 \times 10^{-6} .$$

If it is assumed that the yield is half nickel and half zinc, then 1 at. % of transmuted atoms will change the electrical resistance by the order of 6×10^{-7} ohm-cm, hence the electrical resistivity should increase by the order of 4×10^{-10} ohm-cm as a result of the transmuted atoms. The observed change is an order of magnitude greater than this. Therefore, the observed changes in electrical resistivity are probably the result of displaced atoms. This should be verified experimentally by measuring the resistivity after the hardness changes have been annealed from the single crystal.

It is possible to estimate the number of Frenkel defects formed during a bombardment by means of the change in electrical resistivity. A very crude estimate can be made by assuming that an interstitial atom or an atom vacancy has the same scattering cross section as an impurity ion that

TABLE 10. ELECTRICAL RESISTIVITY OF COPPER CRYSTALS

T = temperature (°C); ρ_T = resistivity at temperature T; $\Delta\rho_T$ = change in resistivity at temperature T.

SAMPLE	TREATMENT	T (°C)	ρ_T (μohm-cm)	ρ_{20} (μohm-cm)	T′ (°C)	$\rho_{T'}$ (μohm-cm)	$\rho_{-196.0}$ (μohm-cm)	$\Delta\rho_{20}$ (μohm-cm)	$\Delta\rho_{-196.0}$ (μohm-cm)
19A	Annealed	18.27	1.6732	1.6846	−196.03	0.19692	0.19712		
		17.58	1.6686	1.6846	−196.01	0.19678	0.19685	0.0000	−0.0003
		15.81	1.6569	1.6847				+0.0001	
	Exposed to	17.48	1.6680	1.6846	−195.91	0.19726	0.19666	0.0000	−0.0005
	3.28×10^8 r	18.19	1.6729	1.6849	−196.01	0.19642	0.19649	+0.0003	−0.0006
	γ rays	12.43	1.6347	1.6848				+0.0002	
21A	Annealed	18.59	1.6731	1.6824	−195.99	0.19922	0.19915		
		20.86	1.6877	1.6819	−196.02	0.19885	0.19898	−0.0005	−0.0002
		17.03	1.6628	1.6825	−196.03	0.19926	0.19945	+0.0001	+0.0003
	Exposed to	13.85	1.6418	1.6825	−196.00	0.19941	0.19941	+0.0001	+0.0003
	3.2×10^8 r	8.28	1.6046	1.6822	−196.11	0.19828	0.19902	−0.0002	−0.0001
	γ rays								
14B	Annealed	19.19	1.6777	1.6830	−195.99	0.20129	0.20107		
		18.53	1.6733	1.6830	−196.02	0.20118	0.20131	0.0000	+0.0002
	After	19.64	1.6855	1.6879	−195.97	0.20608	0.20588	+0.0049	+0.0048
	2×10^{18} nvt	19.77	1.6890	1.6904	−196.04	0.20599	0.20586	+0.0074	+0.0048
		18.94	1.6812	1.6882	−196.07	0.20537	0.20584	+0.0052	+0.0048
		19.96	1.6885	1.6887	−196.02	0.20543	0.20555	+0.0057	+0.0045
		18.72	1.6799	1.6884	−196.03	0.20565	0.20585	+0.0054	+0.0048
		18.31	1.6766	1.6878				+0.0048	
		15.82	1.6631	1.6908				+0.0078	
17A	Annealed	18.43	1.6774	1.6878	−195.98	0.20248	0.20235		
		18.01	1.6748	1.6880	−196.02	0.20222	0.20235	+0.0002	0.0000
	After	19.77	1.6914	1.6929	−196.05	0.20643	0.20677	+0.0051	+0.0044
	2×10^{18} nvt	20.25	1.6946	1.6929	−196.04	0.20640	0.20666	+0.0051	+0.0043
		19.25	1.6892	1.6942	−196.01	0.20677	0.20677	+0.0064	+0.0044
		18.26	1.6822	1.6937	−196.01	0.20680	0.20687	+0.0059	+0.0045
		21.57	1.7043	1.6939				+0.0061	
16A	Annealed	17.80	1.6724	1.6870	−195.99	0.20305	0.20298		
		17.81	1.6726	1.6871	−196.04	0.20269	0.20296	+0.0001	0.0000
	After	20.70	1.6974	1.6928	−196.03	0.20755	0.20755	+0.0058	+0.0048
	2×10^{18} nvt	17.12	1.6745	1.6936	−196.06	0.20720	0.20760	+0.0066	+0.0046
		20.37	1.6955	1.6931	−195.94	0.20755	0.20715	+0.0061	+0.0042

has a nuclear charge of plus or minus one from that of copper. Dexter has recently made a more elegant estimate of the cross section[3] with results that agree in order of magnitude with the latter assumption. Both the estimates ignore the screening that should result in a smaller cross section.

On the basis of Dexter's estimate, 1 at. % of Frenkel defects should result in a change in resistivity of 1×10^{-6} ohm-cm. On the basis of Seitz's computations, Eq. 4, a bombardment of 2×10^{18} nvt should result in 2×10^{-1} % Frenkel

[3] D. L. Dexter, Dept. of Physics, University of Illinois, private communication.

defects, so that a change in resistivity of about 2×10^{-7} ohm-cm should be observed. The observed changes are about two orders of magnitude smaller than this.

Post-irradiation densities of samples *3B*, *T1*, and *T2* are reported in Table 11 with reference to unirradiated sample *3A* in order to remove any systematic errors that may have arisen during the period of bombardment. It is clear from these data that, if there is a change in density due to an exposure of 1×10^{18} nvt, it must be small.

Figure 27 shows stress-strain curves of samples *3A*, *3B*, *T1*, and *T2*. A substantial increase in the critical shear stress resulting from the reactor bombardment is observed in these data, whereas no appreciable change in stress-strain curve as a result of the exposure to gamma rays is observed.

X-RAY WORK

G. E. Klein F. A. Sherrill

A G-E x-ray power supply and control panel have been installed. The entire spectrometer unit has been fitted with special attachments required in the study of rocking-curve data from single crystals of copper.

The installation of the G-E power supply at the spectrometer site permits operation of the G-E x-ray tube at full rating and eliminates the problems previously concerned with the transmission of high voltages over long distances before reaching the x-ray tube itself. The North American Philips unit is now free for operating the two x-ray tubes used in the analysis of normal x-ray problems.

The x-ray studies of copper phthalocyanine, elastomers and plastics, and creep specimens of Inconel are discussed under the groups initiating such work.

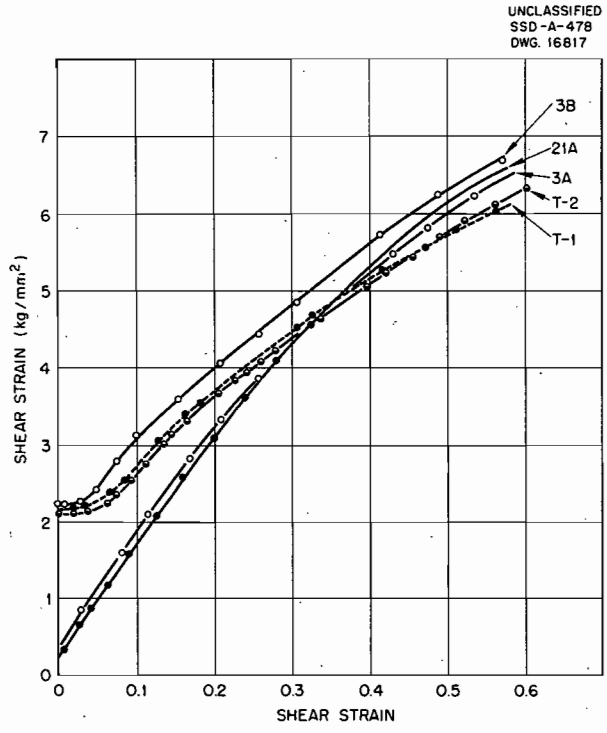

Fig. 27. Stress-Strain Curves for Copper Single Crystals.

TABLE 11. RELATIVE DENSITY* OF COPPER BEFORE AND AFTER IRRADIATION

SAMPLE	TRIAL I	TRIAL II	TRIAL III	AVERAGE
		Before Irradiation		
T1	1.000183	1.000288	1.000382	1.000284 ± 0.000068
T2	1.000261	1.000292	1.000263	1.000272 ± 0.000013
3B	1.000042	1.000121	1.000047	1.000070 ± 0.000034
		After 1×10^{18} nvt		
T1	1.000138	1.000454	1.000269	1.000287 ± 0.000111
T2	1.000219	1.000237	1.000136	1.000197 ± 0.000041
3B	1.000163	1.000029	1.000089	1.000094 ± 0.000046

*Density in reference to a single copper crystal of the same shape as samples that were irradiated.

[redacted]

[redacted]

[redacted]

This doc[redacted]ontains Restricted Data as defined in the Atomic Ene[redacted]ontents in any mann[redacted] is prohibited.

[redacted]

[redacted]